UCSF
UC San Francisco Electronic Theses and Dissertations

Title
Determining Mechanisms of Endochondral Repair in the Craniofacial and Appendicular Skeletons: A Story of Chondrocyte-to-Osteoblast Transformation via Wnt Signaling

Permalink
https://escholarship.org/uc/item/7sw4t6x5

Author
Wong, Sarah Anne

Publication Date
2018

Peer reviewed|Thesis/dissertation

eScholarship.org Powered by the California Digital Library
University of California

Determining Mechanisms of Endochondral Repair in the Craniofacial and Appendicular Skeletons: A Story of Chondrocyte-to-Osteoblast Transformation via Wnt Signaling

by

Sarah Anne Wong

DISSERTATION

Submitted in partial satisfaction of the requirements for degree of

DOCTOR OF PHILOSOPHY

in

Oral and Craniofacial Sciences

in the

GRADUATE DIVISION

of the

UNIVERSITY OF CALIFORNIA, SAN FRANCISCO

Approved:

DocuSigned by:
Tamara Alliston
E233CABEF261499...

Tamara Alliston

Chair

DocuSigned by:
Ralph Marcucio
[illegible]

Ralph Marcucio

DocuSigned by:
Chelsea S Bahney
[illegible]

Chelsea S Bahney

DocuSigned by:
Edward Hsiao
[illegible]

Edward Hsiao

DocuSigned by:
[illegible]
F69F10B7A1234BF...

Mary Nakamura

Committee Members

Dedication

Sarah Anne Wong would like to dedicate this dissertation to the family, friends, and mentors who have supported her throughout her educational journey. She would particularly like to recognize her parents (Anna and Clyde Wong), her sister (Elizabeth Anne Wong), past and present research mentors (Ralph Marcucio, Chelsea Bahney, Katerina Venderova, Marcos Gridi-Papp, Lisa Wrischnik, Mariko Bennett, Ben Barres, Frank Longo, and Andreas Franz), her thesis committee members (Tamara Alliston, Edward Hsiao, Mary Nakamura), and long-time friends (Christie & Keith Yoshikawa, Sandra Austin, Kayla Chun, Sharaya Galbraith, Jessica Westbrook, Audrey Chan, Nina Vilme, Debbie Gray, Christine Hsu, Lydia Foo, Eeva Hall, Ilene Kelsey, Susan Leong, Cris Alcantara, Larry Dahm, Pam Kojimoto, and Kelsey Belomy).

Acknowledgements

Ms. Wong would like to acknowledge the following individuals for their contributions to her research: Drs. Ralph Marcucio, Chelsea Bahney, Tamara Alliston, Edward Hsiao, and Mary Nakamura for their contributions to study design; Diane Hu, Tiffany Shao, Erene Niemi, Emilie Barruet, Blanca M. Morales, Omid Boozarpour, Joshua Slocum, and Michael Nguyen for their advice and assistance in executing experiments; Drs. Theodore Miclau, Ralph Marcucio, Chelsea Bahney, Mary Nakamura, Edward Hsiao, the AO Foundation, the NIH / NIDCR, and the AADOCR for financial support and providing supplies and equipment for these experiments.

Contributions

This dissertation includes excerpts from the following publications:

Chapter 1 / Introduction:

Wong S, Rivera K, Miclau T, Alsberg E, Marcucio R, Bahney C. "Microenvironmental Regulation of Chondrocyte Plasticity in Endochondral Repair – a New Frontier for Developmental Engineering." *Frontiers in Bioengineering and Biotechnology*, section *Tissue Engineering and Regenerative Medicine,* 2018.

Chapter 2:

Wong S, Hu D, Slocum J, Nguyen M, Miclau T, Marcucio R, Bahney C. "Chondrocyte-to-Osteoblast Transformation in Mandibular Fracture Repair." *Journal of Orthopaedic Research*, 2020.

Chapter 3:

Wong S, Hu D, Shao T, Niemi E, Barruet E, Morales B, Boozarpour O, Miclau T, Hsiao E, Nakamura M, Bahney C, Marcucio R. "β-catenin Signaling Regulates Cell Fate Decisions at the Transition Zone of the Chondro-Osseous Junction During Fracture Healing." *bioRxiv*, 2020.2003.2011.986141, doi:10.1101/2020.03.11.986141, 2020.

These publications form the basis of Ms. Wong's dissertation. They were primarily conducted and written by Ms. Wong and are substantially the product of her period of study at UCSF. These publications represent research and scholarship comparable in scope and contribution to a standard dissertation.

Determining Mechanisms of Endochondral Repair in the Craniofacial and Appendicular Skeletons: A Story of Chondrocyte-to-Osteoblast Transformation via Wnt Signaling

Sarah Anne Wong

Abstract

The majority of fracture research has been conducted in long bones with significantly less work done in the craniofacial skeleton. Craniofacial bones differ from long bones in both their developmental mechanism and embryonic origin. Thus, it is possible that their healing mechanisms may differ as well. We sought to determine the regulatory mechanisms that govern fracture repair in both the craniofacial and appendicular skeletons using mandibular and tibial fracture models. Stabilized and unstabilized mandible fracture models were created which heal via intramembranous and endochondral ossification, respectively. Whereas bone forms directly via intramembranous ossification, endochondral ossification occurs through a cartilage intermediate that is gradually replaced with bone. Using our mandible fracture models, we confirmed that mechanical motion promotes robust cartilage formation whereas mechanical stabilization favors intramembranous ossification, a phenomenon previously demonstrated in long bone fractures. Due to the mobility experienced at the fracture site, the majority of clinical fractures heal through the process of endochondral ossification. Recent genetic studies conducted in the appendicular skeleton have demonstrated that during endochondral ossification a significant portion of callus chondrocytes transform into osteoblasts that derive the new bone. Using genetic lineage tracing and immunohistochemistry, we demonstrated that mandibular callus chondrocytes also undergo chondrocyte-to-osteoblast transformation, that they significantly contribute to new bone formation, and that they express pluripotent stem cell (Sox2) and osteogenic (OC) markers while undergoing their transition. Due to the important role of cartilage during fracture repair, we tested the efficacy of using cartilage grafts to heal critical-sized mandibular defects. Cartilage grafts not only produced complete bony-bridging of the defects, but the newly formed bone was

also highly vascularized and primarily derived from donor / graft tissue. Using unstabilized tibial fracture models which heal via endochondral ossification, we sought to determine the molecular signals that regulate chondrocyte-to-osteoblast transformation. We hypothesized that canonical Wnt signaling plays a key role in this process and used loss-of-function and gain-of-function experiments to test our hypothesis. By inhibiting or over-activating the pathway through conditional expression in chondrocytes of a truncated or stabilized form of β-catenin, a key downstream co-factor required for canonical Wnt signaling, we demonstrated that pathway inhibition leads to impaired bone formation whereas pathway overstimulation results in osteopetrotic bone. Interestingly, inhibition of canonical Wnt signaling did not significantly increase chondrocyte cell death. Rather chondrocytes remained as detached cells in the marrow space. Additionally, global inhibition of Wnt ligand palmitoylation, a key step in ligand packaging and release, through conditional Porcupine deletion did not significantly inhibit chondrocyte-to-osteoblast transformation. Thus, although canonical Wnt signaling plays a key role in chondrocyte-to-osteoblast transformation during endochondral repair, this process appears to be independent of Wnt ligands modified via Porcupine-mediated palmitoylation. These data confirm that chondrocyte-to-osteoblast transformation occurs in both the craniofacial and appendicular skeletons, that canonical Wnt signaling plays a critical role in regulating chondrocyte transformation, and that this process is independent of Wnt ligands palmitoylated via Porcupine. Moreover, these data lend key insight into the development of novel and improved fracture therapies including the use of cartilage as a graft alternative for craniofacial fractures.

Table of Contents

List of Figures

List of Tables

Chapter 1:

Introduction

Fractures heal through two pathways: endochondral ossification and intramembranous ossification.[1,2] Both processes begin with the differentiation of local osteochondral progenitor cells found within the periosteum and endosteum.[3,4] During endochondral ossification, or indirect bone healing, progenitor cells primarily derived from the periosteum differentiate into chondrocytes to form a cartilage callus between the fractured bone ends.[4] This cartilage is gradually replaced with bone in a process that resembles embryonic bone development and postnatal growth. Intramembranous ossification, or direct bone healing, occurs when periosteal and endosteal progenitor cells differentiate directly into osteoblasts. Fate of the osteochondral progenitor is determined by the relative stability of the fracture site, with motion stimulating endochondral ossification and rigid microenvironments promoting intramembranous ossification.[2] In most cases, both healing pathways occur simultaneously such that a robust cartilage callus forms at the center of the fracture where the degree of motion is greatest, and intramembranous bone forms along the periosteal and endosteal surfaces.[2] Endochondral ossification is the predominant mechanism by which the majority of fractures heal and is the focus of this dissertation.[1,5]

Formation of the cartilage callus functionally serves to stabilize the gap between the bone ends. To form the cartilage callus, periosteal osteochondral progenitor cells migrate from the periosteum and undergo chondrogenic differentiation.[3] This occurs on top of the provisional fibrin matrix formed by the hematoma.[6] Growth factors produced by the hematoma promote cell migration and differentiation and also create a unique microenvironment with low pH and high lactate concentration.[7] Formation of the hematoma and a strong pro-inflammatory response are essential to establishing a robust healing response.[8]

Following the initial hematoma, subsequent steps of chondrogenesis and chondrocyte hypertrophy appear to parallel the molecular pathways involved in endochondral ossification in the growth plate during bone development.[9,10] Chondrogenic programming is initiated by the expression of transcription factor Sox9, which is required for chondrogenesis.[11,12] Sox9 regulates the expression of several chondrocyte-specific matrix components including collagen type II and aggrecan, the two predominant proteins within the cartilage matrix.[13,14] This initial extracellular matrix is avascular and aneural until blood vessels and nerves penetrate the soft callus during later stages of healing.[15–18] As chondrocytes mature, they produce collagen type X, mineralize their surrounding matrix, and undergo hypertrophy, increasing in volume and mass by ~20-fold.[19]

There has been a centuries-long debate regarding the subsequent fate of hypertrophic chondrocytes during endochondral bone development and repair. In the early 1800's, cartilage was believed to turn into bone.[20] However, in the mid-1800's, Muller and Sharpy changed this paradigm by claiming that chondrocytes are terminally-differentiated and ultimately undergo cell death, resulting in the replacement of cartilage with bone derived from a separate population of cells.[20] The latter model of chondrocyte fate, for the most part, dominated in textbooks and became the *de facto* model. In recent years, modern murine genetics has enabled lineage tracing studies that more accurately follow the fate of cells. Using a combination of over five different genetic models, evidence now demonstrates that a significant portion of chondrocytes survive, proliferate, and transform into osteoblasts that derive the new bone.[17,22–27]

Pathways that regulate chondrocyte-to-osteoblast conversion have practical implications on fracture healing. Importantly, since conversion of cartilage to bone is necessary for bone regeneration, it is critical to understand the molecular mechanisms regulating this process. Not only will these mechanistic data improve our understanding of impaired healing, especially in the

context of hypertrophic nonunions where cartilage fails to convert to bone, but they will also enable new opportunities for therapeutic intervention through modulation of chondrocyte transformation.

FRACTURE HEALING STANDARD OF CARE

Bone Grafting

Surgical intervention is currently the only effective treatment option for recalcitrant fractures.[1] Standard of care is to use bone autograft or allograft to stimulate healing.[28] Together this makes bone the second-most commonly transplanted tissue behind blood. While bone autografts stimulate strong bone repair, they come with the cost of significant donor site morbidity and limited supply. On the other hand, while bone allografts are readily available, they have significantly reduced bioactivity resulting in clinical failure associated with poor osteointegration and osteonecrosis of the graft.[29] Consequently, there is an unmet clinical need to develop pharmacologic agents that can be used either as a non-invasive alternative or in conjunction with surgical treatment to stimulate endogenous healing mechanisms and improve fracture outcomes.

Bone Morphogenetic Proteins

Bone morphogenetic proteins (BMPs) are currently the most common clinically-used biologics. BMP signal transduction occurs through the binding of BMP ligands to type I and type II serine/threonine kinase receptors (BMPR-I, BMPR-II). This induces phosphorylation of BMP receptors and subsequent phosphorylation of receptor SMADS (R-SMADs) 1, 5, and 8. R-SMADS then form a complex with SMAD4, enabling it to enter the nucleus where it regulates gene expression **(Figure 1.1)**.[10,30,31]

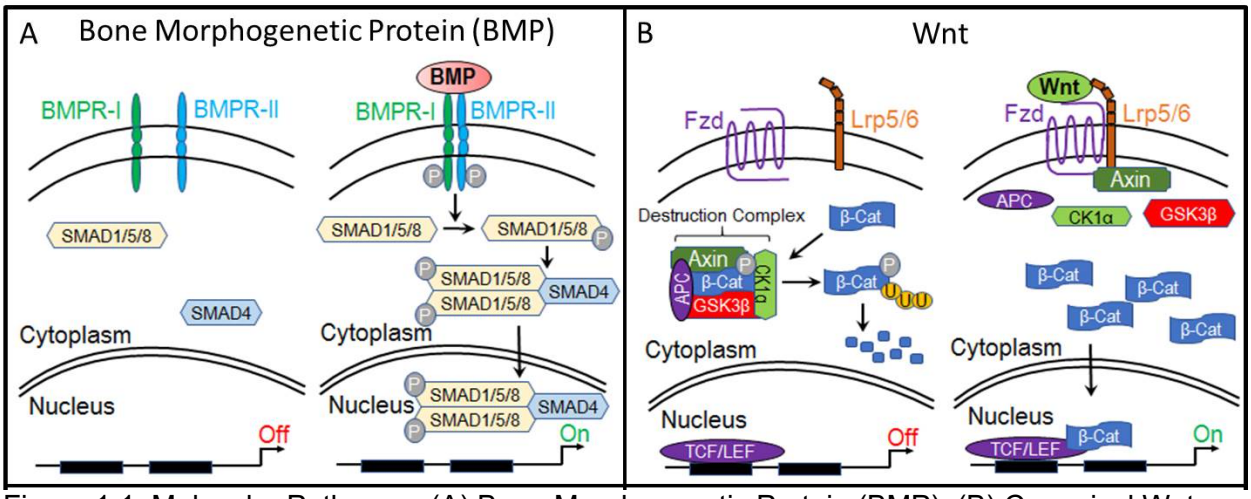

Figure 1.1: Molecular Pathways. (A) Bone Morphogenetic Protein (BMP), (B) Canonical Wnt.

Pre-clinical studies indicated that the BMP pathway was an excellent target for therapeutic development due to its role in regulating osteoblastogenesis and the ability of several BMPs to strongly induce bone formation.[32–34] This led to a series of clinical trials and FDA approval of two recombinant BMPs. Recombinant human BMP2 (INFUSE®) obtained pre-market approval for use in lumbar spinal fusion and for the treatment of compound tibial fractures.[32,35] Recombinant human BMP7, also known as Osteogenic Protein 1 (OP-1), received a Humanitarian Device Exemption for the treatment of recalcitrant long bone nonunions and for revisions of lumbar spinal fusions.[32,35] However, although rhBMP2 has exhibited clinical success in spinal fusion, both rhBMP2 and rhOP-1 have shown less impressive results in the treatment of fracture nonunions.[32] rhOP-1 has now been taken off the market and use of rhBMP2 has been significantly diminished as a result of reports of serious side effects, including heterotopic ossification and tumorigenesis, and by the expense of treatment ($5,000-$15,000 per treatment).[32,35–37]

It has been postulated that the lack of clinical success with BMPs is due to limited understanding of the molecular signals responsible for regulating fracture repair and that a combination of biologics applied during the appropriate phases of the repair process will be required to effectively

stimulate healing.[38–40] Supraphysiological dosing, burse release kinetics, and rapid diffusion of BMPs are also key factors contributing to heterotopic ossification.[41]

NOVEL MOLECULAR TARGETS FOR FRACTURE HEALING

Numerous studies have identified new molecular targets that may regulate chondrocyte-to-osteoblast transformation during endochondral repair. Hu *et al.* defined the chondro-osseous border in the fracture callus where chondrocyte transformation occurs as the "Transition Zone."[17] In this region, mature hypertrophic chondrocytes express classic osteogenic markers (i.e. runx2, osterix, collagen type I, osteocalcin, osteopontin) indicating that these cells adopt an osteogenic fate.[17] Interestingly, Hu *et al.* also demonstrated that hypertrophic chondrocytes at the Transition Zone express pluripotency transcription factors Sox2, Oct4, and Nanog, suggesting that chondrocytes acquire a stem cell-like state during transformation.[17] Sox2 was shown to play an important role during chondrocyte transformation since its deletion resulted in significantly reduced bone formation and increased cartilage retention within the fracture callus.[17]

Despite advances in our understanding of chondrocyte gene expression during transformation, the signaling mechanisms that direct this process remain largely unknown. Evidence suggests numerous molecular pathways as regulatory candidates, including canonical Wnt.

Canonical Wnt Signaling

Wnt signaling is traditionally categorized into the β-catenin-dependent canonical pathway and the β-catenin-independent non-canonical pathways (planar cell polarity and Ca^{2+}-mediated pathways).[42] While some evidence suggests that the non-canonical pathways may play a role in regulating osteogenesis, the canonical Wnt/β-catenin pathway is the most studied and has been shown to play a dominant role in bone development and fracture repair. [43]

The primary function of canonical Wnt signaling is to regulate the transcription of genes involved in cellular processes such as proliferation, differentiation, self-renewal, and survival. When this pathway is inactive, β-catenin, a transcriptional co-activator and the primary effector of this pathway, is bound by a multiprotein "destruction" complex, which consists of Axin, adenomatous polyposis coli (APC), and serine/threonine kinases glycogen synthase kinase 3β (GSK3β) and casein kinase 1α (CK1α). This destruction complex phosphorylates β-catenin, targeting it for ubiquitination and ultimately proteosomal degradation. However, when the pathway is activated by the binding of Wnt ligands to Frizzled and LRP5/6 receptors, the destruction complex is disrupted, enabling β-catenin to accumulate within the cytoplasm and translocate to the nucleus, where it interacts with members of the T-cell factor/lymphocyte elongation factor (TCF/LEF) family to activate transcription of target genes **(Figure 1.1)**.[42]

The canonical Wnt pathway has an established role in osteogenesis and skeletal formation by functioning as a molecular switch regulating lineage commitment between osteogenesis and chondrogenesis.[44,45] During development, inhibition of canonical Wnt signaling through conditional deletion of β-catenin from limb and head mesenchyme using *Prx1*-CreERT, or conditional deletion from skeletogenic mesenchyme using *Dermo1*-Cre, inhibits bone formation and results in early osteoblast differentiation arrest.[44,46] Osteoblastogenesis halts at the osteochondral progenitor stage and cells differentiate into chondrocytes, resulting in the formation of ectopic cartilage.[44,46] Although cells express Runx2, an early marker of the osteoblast lineage, they fail to express osterix, indicating that these cells are incapable of committing to an osteogenic fate.[44,46] *In vitro* experiments inhibiting canonical Wnt signaling in mesenchymal progenitor cells provide similar findings.[44]

Canonical Wnt signaling also plays a key role in directing osteogenesis during intramembranous repair.[47] Using a transcortical defect model, which heals through intramembranous ossification,

inhibition of Wnt signaling through adenoviral expression of Dkk1 prevented the differentiation of osteoprogenitor cells into osteoblasts and significantly reduced bone regeneration compared to controls.[47] Conversely, activating the canonical Wnt pathway through deletion of pathway inhibitors (sclerostin or Axin2) significantly improved intramembranous bone formation.[48] Furthermore, treatment of bone grafts with Wnt3a protein restored the osteogenic potential of aged bone grafts and promoted intramembranous healing of critical-sized defects in mouse calvaria and rabbit ulna.[49]

Less work has been done to determine the role of canonical Wnt signaling during endochondral bone formation and repair since traditionally the Wnt pathway is thought to promote direct osteogenesis. However, the mounting data demonstrating chondrocytes can directly form bone in development and repair suggests that canonical Wnt signaling may have a functional role in chondrocyte-to-osteoblast transdifferentiation.[17,22–27] This was directly tested recently by Houben *et al.* who showed that conditional deletion of β-catenin in *col10a1*-expressing hypertrophic chondrocytes resulted in significantly reduced bone, whereas stabilized β-catenin produced osteopetrotic tissue during endochondral development.[24]

Since fracture repair in many ways recapitulates bone development, canonical Wnt signaling may play a similar role in regulating chondrocyte-to-osteoblast transformation during endochondral repair. Indeed, during endochondral healing, nuclear localization of β-catenin was seen in hypertrophic chondrocytes at the fracture callus Transition Zone, indicating that these cells undergo active canonical Wnt signaling.[17] RT-qPCR analysis of fracture calli revealed that numerous Wnt ligands, receptors, and transduction machinery are expressed during fracture repair.[43,50] Huang *et al.* demonstrated that inhibition of Wnt/β-catenin signaling in chondrocytes, using an 82-amino-acid peptide called Inhibitor of β-catenin/TCF (ICAT) driven by *col2a1* expression, delayed cartilage formation and reduced bone formation.[51] Similarly, activation of

canonical Wnt signaling through treatment with lithium chloride enhanced bone formation.[43] Interestingly, enhanced bone regeneration was only observed when the Wnt pathway was activated at later time points, which corresponds biologically with chondrocyte-to-osteoblast transformation.[43] Together, these data suggest that canonical Wnt signaling may play a role in regulating chondrocyte-to-osteoblast transformation during fracture healing.

The evidence outlined above are derived primarily from pre-clinical studies and *in vitro* systems. However, it is likely that the canonical Wnt pathway plays a similarly critical role in humans. Numerous human bone diseases are associated with mutations to components of the canonical Wnt pathway.[52] Predisposition to osteoporosis has been associated with genomic polymorphisms in or close to Wnt/β-catenin signaling components.[52] Loss-of-function mutations in the Wnt receptor LRP5 are associated with osteoporosis pseudoglioma (OPPG) syndrome and juvenile osteoporosis and gain-of-function mutations in the same receptor result in the opposite phenotype of high bone mass and enhanced bone strength.[32,52] Sclerosteosis is a bone disease characterized by an overgrowth of bone and is caused by mutations in the gene and enhancer regions of the Wnt/β-catenin antagonist *sclerostin* (*SOST*).[32,52] Furthermore, the canonical Wnt pathway has been implicated in the context of human fracture repair since β-catenin and sclerostin levels have been shown to increase.[43,53]

The canonical Wnt pathway is primed for translation. Numerous Wnt pathway regulators are being developed and several are already in clinical trials. The majority of these pathway modulators serve to activate the canonical Wnt pathway by neutralizing pathway inhibitors such as Dkk1 and sclerostin.[54] This indirect approach to pathway activation has been adopted primarily because direct pathway activation through treatment with Wnt ligands is clinically-irrelevant. Endogenous Wnts are hydrophobic due to palmitoylation, a form of lipidation required for the intracellular trafficking and full activation of Wnts.[55–57] This makes Wnts challenging to extract and purify,

requires that they be delivered using special liposome-based systems, and significantly increases the cost of treatment.[58] Fortunately, several of the Wnt pathway modulators acting to neutralize pathway inhibitors have shown promising osteogenic effects during clinical trials.

Romosozumab is one such Wnt pathway modulator that received FDA approval in April 2019. It is a humanized monoclonal antibody that binds to and neutralizes the Wnt inhibitor sclerostin.[54] Studies show that treatment with Romosozumab significantly increases bone mineral density and reduces incidence of osteoporotic fractures.[54] Wnt pathway regulators, such as Romosozumab, could readily be repurposed for the context of fracture repair. However, the optimal dosage, timing, and the method of treatment still need to be determined.

VASCULATURE REGULATION OF CHONDROCYTE-TO-OSTEOBLAST TRANSFORMATION

The vasculature plays a critical role during fracture repair. Whereas the normal rate of impaired healing is 10-15%, this percentage increases to 46% when fractures occur in conjunction with severe vasculature injury.[1] The role of the vasculature begins at the outset of injury during hematoma formation where it helps to create the growth factor rich fibrin blood clot upon which periosteal stem cells differentiate to chondrocytes under a low pH, high lactate microenvironment.[6,7] After chondrogenic differentiation, the cartilage anlage is avascular and chondrogenic maturation happens in the absence of a regulatory role from the vasculature.[15,17,18]

In the later stages of repair, blood vessels are recruited into the cartilage fracture callus by hypertrophic chondrocytes expressing vascular endothelial growth factor (VEGF) and placental growth factor (PlGF).[15,17,59,60] Histologically, the cartilage-to-bone transition in the fracture callus occurs around this invading vasculature.[17] Importantly, spatiotemporal expression of osteogenic genes and pluripotency transcription factors occurs in hypertrophic chondrocytes adjacent to the vasculature, suggesting that the vasculature plays a role in initiating chondrocyte transformation.[17]

Growth Factor Secretion

Endothelial cells from the vasculature may functionally contribute to phenotypic modulation of the chondrocyte phenotype through secretion of pro-osteogenic growth factors. For example, it has been established that vascular tissues are a direct endogenous source of BMPs.[61,62] Functionally it has been shown that secreted factors from vascular endothelial cell conditioned media were capable of inducing matrix mineralization and up-regulating the classic osteogenic gene *osteocalcin.*[23] It is likely that BMP expression contributed to this phenotype.[23] However, more recently it was also shown that the same vascular endothelial cell conditioned media induced expression of pluripotency transcription factors (Sox2, Oct4, Nanog) indicating that an additional factor may have a role in activating a stem-like state.[17] While the complete secretome of vascular endothelial cells during fracture healing has not been detailed, it is known that this secretome is site specific.[63,64] It is possible that fracture callus endothelial cells secrete factors other than BMP that may play a role in directing osteogenesis or chondrocyte plasticity.

DEVELOPMENTAL ENGINEERING TO RECAPITULATE ENDOCHONDRAL OSSIFICATION

While the established clinical approaches to bone regeneration promote intramembranous bone formation, bones both develop and heal through the process of endochondral ossification during which the cartilage callus creates an angiogenic and osteoconductive scaffold for bone formation. Recent preclinical studies have capitalized on this, proposing therapeutic strategies that parallel the natural healing process by utilizing engineered hypertrophic cartilage grafts to stimulate bone regeneration.[23,65–72] Translating these preclinical studies may improve clinical outcomes.[73]

Further, new mechanistic understanding of endochondral ossification could have a significant impact on the design of novel therapeutics for fracture healing and bone regeneration. Since we now understand chondrocytes can be a direct precursor of osteoblasts, stimulating transformation of chondrocytes into osteoblasts becomes a clinically-relevant therapeutic approach.[17,22,25–27]

Very little work has been done to understand *how* chondrocytes become osteoblasts during endochondral ossification. If we understood the extrinsic mediators of chondrocyte to osteoblast transformation, we would not only be able to engineer an ideal treatment for hypertrophic nonunions, but we could also accelerate fracture healing under normal conditions.

For my dissertation, I sought to identify mechanisms of endochondral repair in the craniofacial and appendicular skeletons and to apply these discoveries to the development of novel therapies. The following two chapters summarize this work.

Chapter 2:

Chondrocyte-to-Osteoblast Transformation in Mandibular Fracture Repair

Craniofacial bones differ from appendicular bones in both their embryonic origin and developmental mechanism.[74] Appendicular bones are derived from lateral plate mesoderm through the process of endochondral ossification. This process begins with the differentiation of mesenchymal stem cells into chondrocytes that form a cartilage template in the approximate size and shape of the future bone. As the skeleton develops, this cartilage anlage is converted to bone. In contrast, craniofacial bones develop from the cranial neural crest through the process of intramembranous ossification. Unlike its counterpart, this process does not involve a cartilage intermediate. Rather, osteochondral progenitors directly differentiate into osteoblasts and form bone.[74] The majority of mechanistic fracture research has focused on long bone fractures in the appendicular skeleton. Given the significant developmental difference between craniofacial and long bones, it is possible that these bones differ in their healing mechanisms as well.

The mandible is one of the most commonly-fractured craniofacial bones, sustaining up to 70% of all maxillofacial fractures.[75] Its daily functional requirement and esthetic role necessitate the development of new and improved therapies. Although the mandible develops via intramembranous ossification, it has been shown to heal via both intramembranous and endochondral ossification.[76] Here we utilized two mandible fracture models: a stabilized trephine defect model that heals via intramembranous ossification, and an unstabilized osteotomy that heals via endochondral ossification. These models were used to determine the role of chondrocyte-to-osteoblast transformation during mandible fracture repair and to test the efficacy of using cartilage grafts to heal mandibular defects.

MATERIALS AND METHODS:

Fractures

All studies were approved by the UCSF Institutional Animal Care and Use Committee and the results have been reported according to ARRIVE guidelines. The following mice were obtained from Jackson Labs and maintained in our colony: C57BL/6J (Stock #: 000664), Aggrecan-Cre^{ERT2} (Stock #: 019148), tdTomato HZE (Stock #: 007909), Rosa26 (Stock #: 002073), Nu/J (Stock #: 002019). Mice were anesthetized with a 1:1 mixture of ketamine (60 mg/kg) and dexmedetomidine (0.3 mg/kg) delivered intraperitoneally (IP). Mandible fractures with different levels of stability were generated in adult (10-16 week) male mice by creating either 1) an unstable osteotomy through the right mandibular ramus from the anterior border of the coronoid process to the anterior border of the angular process or 2) a 1mm-diameter trephine defect through the right mandibular ramus. Animals were randomly assigned to fracture group, and the fracture site location was confirmed via radiography. Animals were revived using an atipamezole reversal agent (6 mg/kg, IP) and were given subcutaneous buprenorphine analgesic (0.05-0.1 mg/kg) immediately post-op, and at 4 and 24 hours post-fracture. Animals received prophylactic antibiotic for up to 5 consecutive days following surgery (25 mg/kg cefazolin or 15 mg/kg enrofloxacin, both IP). All animals in this study were healthy with an average body weight of 23g (20-26g). Any animals displaying signs of infection were excluded from this study. Animals were fed a soft food diet for 7 days and monitored closely for pain and weight loss. Mice were socially housed (up to 5 animals per cage) on a 12-hour light/dark cycle, and allowed to ambulate freely until experimental endpoints. All mice were euthanized with CO_2.

Histology

Mandibles were harvested 7, 10, or 21 days post-operatively and fixed for up to 24 hours at 4°C in 4% paraformaldehyde (PFA, pH 7.4), decalcified for four weeks using 19% ethylenediaminetetraacetic acid (EDTA, pH 7.4), paraffin-embedded and sectioned (10 μm).

Standard histological staining protocols were used to visualize cartilage and bone at each time point: Hall Brunt Quadruple (HBQ, bone stains red, cartilage stains blue); Safranin-O/Fast Green (cartilage stains red, green counterstain). N=5/time point/fracture type.

Immunohistochemistry

Immunohistochemistry for Sox2 (Abcam, ab107156, 1:250) and Osteocalcin (OC, Abcam, ab93876, 1:250) was performed on paraffin-embedded sections of samples harvested 10 days post-fracture (N>5 per antibody). The basic protocol included antigen retrieval in 10 mM sodium citrate buffer (20 min, 100°C), endogenous peroxidase blocking in 3% H_2O_2 (30 min, room temperature) and non-specific epitope blocking with 5% goat serum (GS, 1 hour, room temperature). Primary antibodies were applied to sections overnight at 4C. An HRP-conjugated, species-specific secondary antibody (Millipore, AB307P, 1:200 in PBS with 5% GS, 1 hour, room temperature) was detected using 3,3'-diaminobenzidine (DAB) colorimetric reaction.

Lineage Tracing

Aggrecan-Cre^{ERT2} and tdTomato HZE mice were bred so that their progeny were heterozygous for Cre and tdTomato reporter alleles. Genotype was confirmed through gel electrophoresis according to Jackson Lab's protocols. Unstable mandible fractures were created as above. Cre recombination was induced with daily injections of Tamoxifen (75 mg/kg) from days 6-10 post-fracture, as previously.[17] This recombination period aligned with the peak of the soft, cartilaginous phase of mandibular fracture repair. Samples were harvested 14 days post-fracture, fixed and decalcified as above, cryoembedded, and sectioned (10 μm). Samples were mounted in VectaShield with DAPI (Vector, H-1200) and visualized with an epifluorescence microscope. N=5.

Cartilage Grafts

Critical-sized defects were created in the right mandibular ramus of immunocompromised Nu/J mice either by creating two parallel osteotomies 1.5 mm apart or by drilling a 2 mm-diameter trephine defect through the right mandibular ramus. Defects were filled with cartilage harvested from tibia fracture calli of eGFP or Rosa26 reporter mice 7 days post-fracture as previously.[23] Control defects were left empty. Mandibles were harvested for analysis 7, 14, and 28 days post-engraftment. Progression of healing was assessed via standard histology staining (HBQ) as above. Donor versus host-derived bone was determined via X-gal staining. N=6/time point.

RESULTS:

Mandible fracture models produce distinct reparative patterns

Unstable fractures were generated by creating a complete osteotomy through the right mandibular ramus from the anterior border of the coronoid process to the anterior border of the angular process **(Figure 2.1, A)**. Stable fractures were created by drilling a 1 mm-diameter trephine defect through the right mandibular ramus in an anatomically similar location as the unstable osteotomy **(Figure 2.1, B)**. Fractures were harvested at multiple time points (days 7, 10, and 21 post-fracture) and stained for Hall Brunt Quadruple (HBQ) or Safranin-O (Saf-O) histology to identify cartilage and bone tissues **(Figure 2.1, C-N)**. Whereas unstable fractures developed a robust cartilage callus by 10 days post-fracture, stable fractures exhibited little to no cartilage at all time points **(Figure 2.1, E-F, I-N).** In some instances, small amounts of cartilage were found in the stabilized model outside the defect site, usually ventral and anterior to the defect **(Figure 2.1, K, yellow arrowhead)**. We believe these regions of cartilage are most-likely due to motion derived from residual bone chips left behind from drilling the trephine defect. Indeed, although the fracture site was flushed multiple times with saline following trephine drilling, bone chip remnants were observed adjacent to the fracture site and were often surrounded by small regions of cartilage staining positive for Alcian blue. Unstabilized fractures reached complete bony-bridging by 21

days post-fracture **(Figure 2.1, G-H)**, and stabilized fractures were completely bridged by 10 days post-fracture **(Figure 2.1, K-L)**.

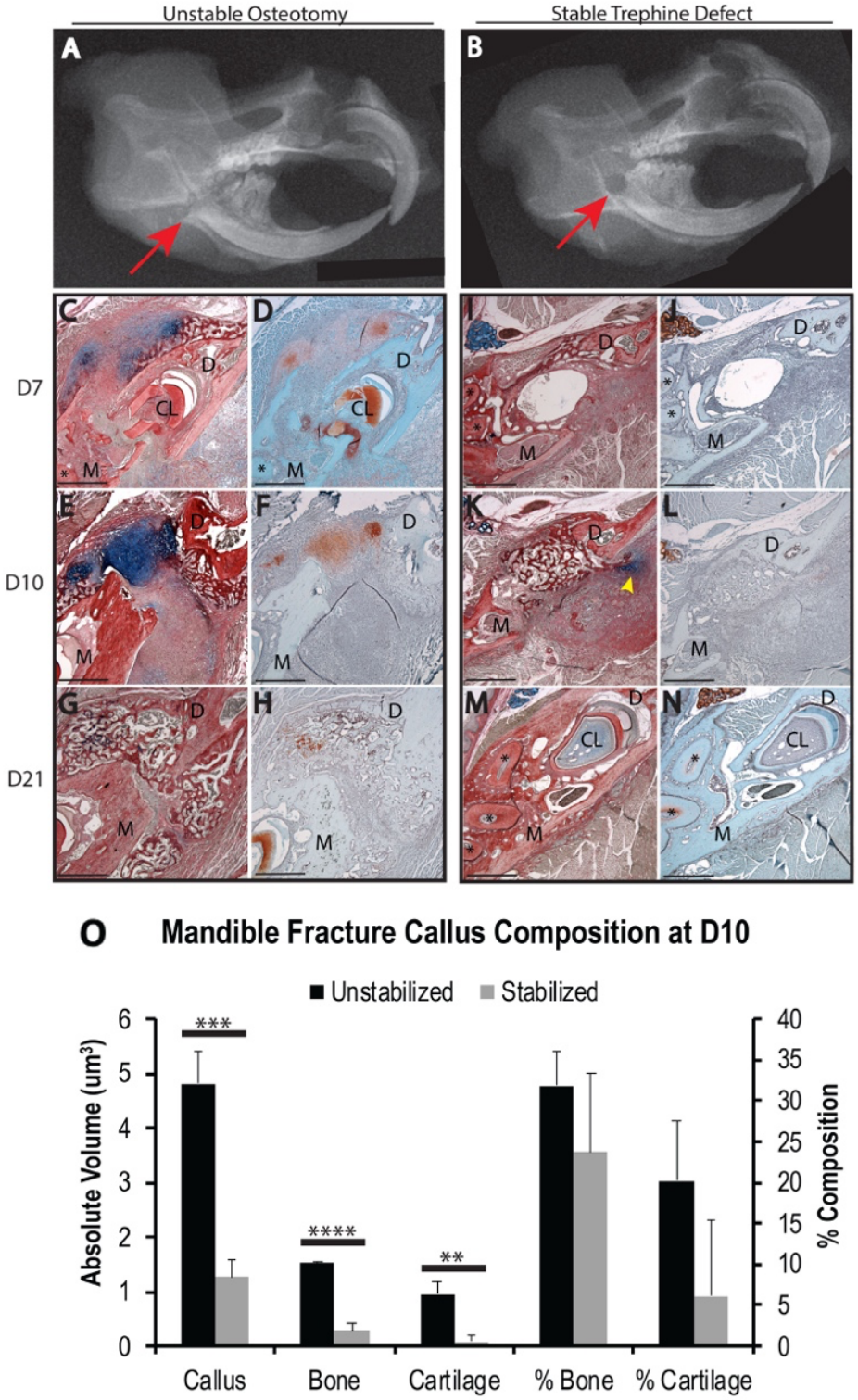

Figure 2.1: Fracture stability mediates mandibular ossification mechanisms. X-ray images of an unstable transverse osteotomy (A) and stable 1 mm trephine defect (B) confirm the proper

anatomical location of fracture site (red arrow) within the right mandibular ramus of C57BL/6 mice. Mandibles were imaged at 7 days post-fracture ($N = 5$/group). HBQ (C, E, G, I, K, M) and Saf-O (D, F, H, J, L, N) standard histology staining of transverse sections reveals that mandibles with unstable osteotomies (C–H) develop a robust cartilage callus and primarily heal through endochondral ossification, whereas mandibles with stable trephine defects (I–N) develop little to no cartilage and primarily heal through intramembranous ossification. Small amounts of cartilage were found adjacent to the fracture site in the stabilized fracture model at 10 days post-fracture, usually ventral and posterior to the defect (K, yellow arrowhead). Cartilage was only observed in the stable fracture model at day 10 post-fracture and was most-likely due to motion derived from residual bone chips left behind from drilling the trephine defect. Stereological analysis of callus tissue composition confirmed that the absolute volume of cartilage was significantly less in stable than in unstable fractures at D10, which is the time point during which the greatest amount of cartilage was observed in either model (O). Complete bony-bridging was observed in the unstable model at D21 postfracture (G, H) and in the stable model at D10 postfracture (K, L). HBQ: cartilage is blue, bone is red. Saf-O: cartilage is red, bone is teal. (*) in histology = mandibular molar roots. $N = 5$/time point/fracture type. Scale = 500 μm. $^{**}p < .01$. $^{***}p < .001$. $^{****}p < .0001$. CL, cervical loop; D, distal; HBQ, hall brunt quadruple; M, mesial; Saf-O, Safranin-O.

Mandibular Chondrocytes Transform into Osteoblasts during Endochondral Repair:

The unstabilized mandible fracture model was used to assess the role of chondrocyte-to-osteoblast transformation during mandibular endochondral repair. Samples were analyzed at 14 days post-fracture, the time point during which significant cartilage-to-bone replacement occurs. Chondrocyte lineage tracing was performed using a tdTomato reporter expressed under the control of a cartilage-specific, inducible Aggrecan-Cre^{ERT2} promoter. The vast majority of chondrocytes within the fracture callus were positive for tdTomato, indicating that Cre-recombination was highly efficient **(Figure 2.2, C)**. Robust tdTomato expression was also observed in osteoblasts and bone-lining cells within the newly formed bone, demonstrating that these cells were chondrocyte-derived **(Figure 2.2, F).** Low magnification images of the Transition Zone region, where callus cartilage joins the newly-formed bone, indicate that the new bone is highly vascularized and that chondrocytes contribute significantly to new bone **(Figure 2.2, A-E)**.

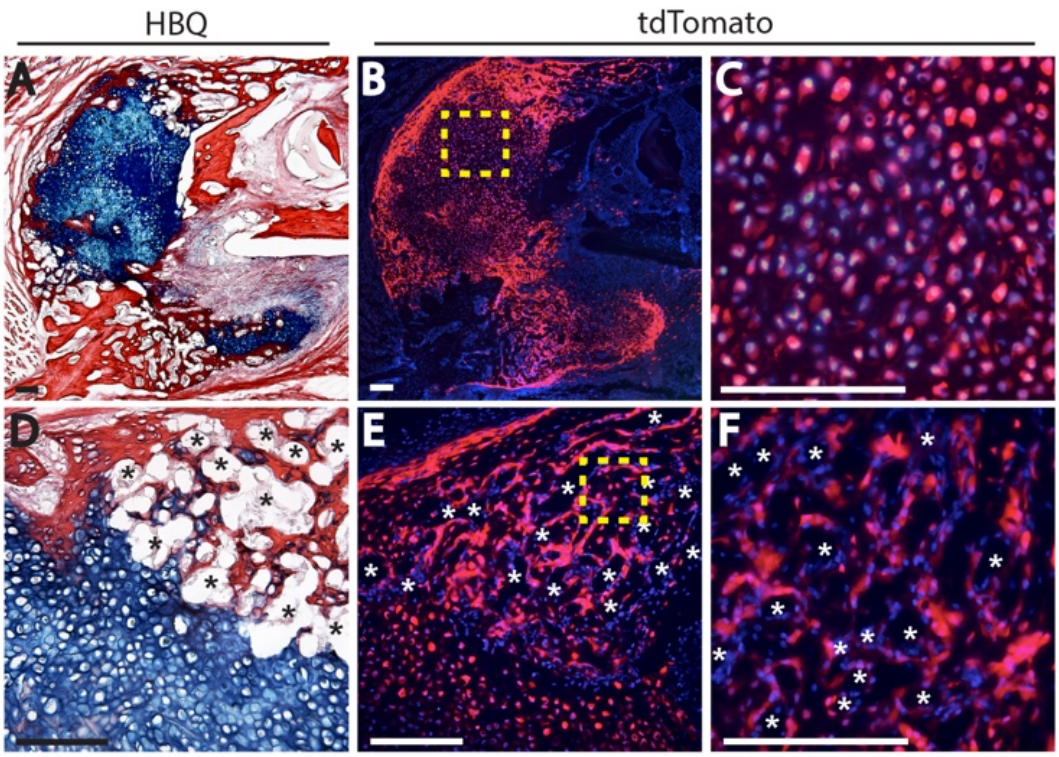

Figure 2.2: Fracture Callus Chondrocytes Give Rise to Osteoblasts and Bone-Lining Cells during Mandibular Endochondral Repair. Lineage tracing of mandibular fracture callus chondrocytes was performed using the Aggrecan-Cre^{ERT2} driver to induce cartilage-specific Cre recombination in the stop-floxed tdTomato reporter mouse. Fluorescence microscopy indicates robust tdTomato expression in chondrocytes within the fracture callus indicating highly-efficient Cre recombination (C, boxed region in B). Robust tdTomato expression is also observed in osteoblasts/cytes within the newly-formed bone and in bone-lining cells, confirming their chondrocyte-derivation (F, boxed region in E). Low-magnification images demonstrate the significant contribution of chondrocytes to new-bone formation (A, D correspond to B, E). DAPI counterstain was used to visualize nuclei (blue). (*) = Blood Vessels. N=5. Scale=100 μm.

Mandibular Callus Chondrocytes in the Transition Zone Express Stem Cell Markers:

The greatest amount of callus cartilage was observed in unstable mandible fracture samples harvested 10 days post-fracture with a robust Transition Zone observed in all samples **(Figure 2.3, A-B)**. Immunohistochemistry revealed that hypertrophic chondrocytes found within the Transition Zone express the transcription factor Sox2 and the ossification marker Osteocalcin **(Figure 2.3, D, F)**. Strong expression of these genes was only observed in hypertrophic chondrocytes at the Transition Zone region. Pre-hypertrophic chondrocytes either did not express these markers or expressed them at much lower levels **(Figure 2.3, C, E)**.

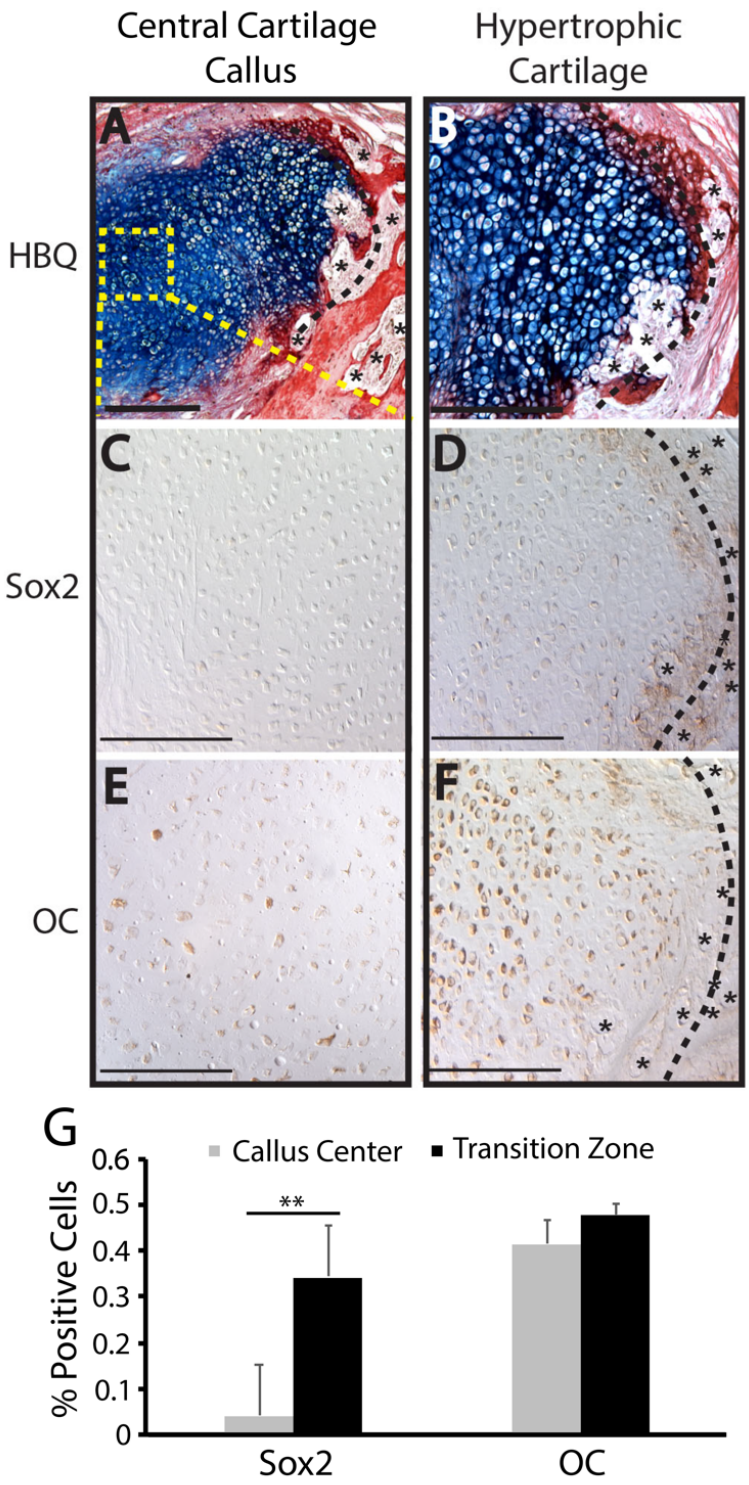

Figure 2.3: Hypertrophic Chondrocytes at the Mandibular Fracture Callus Transition Zone Express Stem Cell and Osteogenic Markers. C57BL/6 mandibles were given unstable osteotomies and harvested 10 days post-fracture. Hall Brunt Quadruple/HBQ (A-B) histology shows robust transition zone (TZ, black dotted line) region within the fracture callus, marked by newly formed blood vessels (*) of the invading vasculature at the chondro-osseous junction. Immunohistochemical analysis demonstrates that hypertrophic chondrocytes at the TZ express

stem cell marker *Sox 2* (D) as well as the classic osteogenic marker *Osteocalcin* (F). Pre-hypertrophic chondrocytes distant from the TZ (boxed region in A) either do not express these genes or express at a significantly lower level (C, E). HBQ: cartilage is blue, bone is red. N=5. Scale=200 μm.

Cartilage Grafts Promote Bone Regeneration in Critical-Sized Mandibular Defects:

Due to the important role of chondrocytes during mandibular endochondral repair, we tested the ability of cartilage grafts to heal critical-sized mandibular defects using two different models: 1) an unstable 1.5 mm defect created by making two parallel osteotomies and 2) a stable 2mm-diameter trephine defect. Defects were confirmed to be critical-sized since no bony bridging was observed in empty defect controls for either model **(Figure 2.4)**.

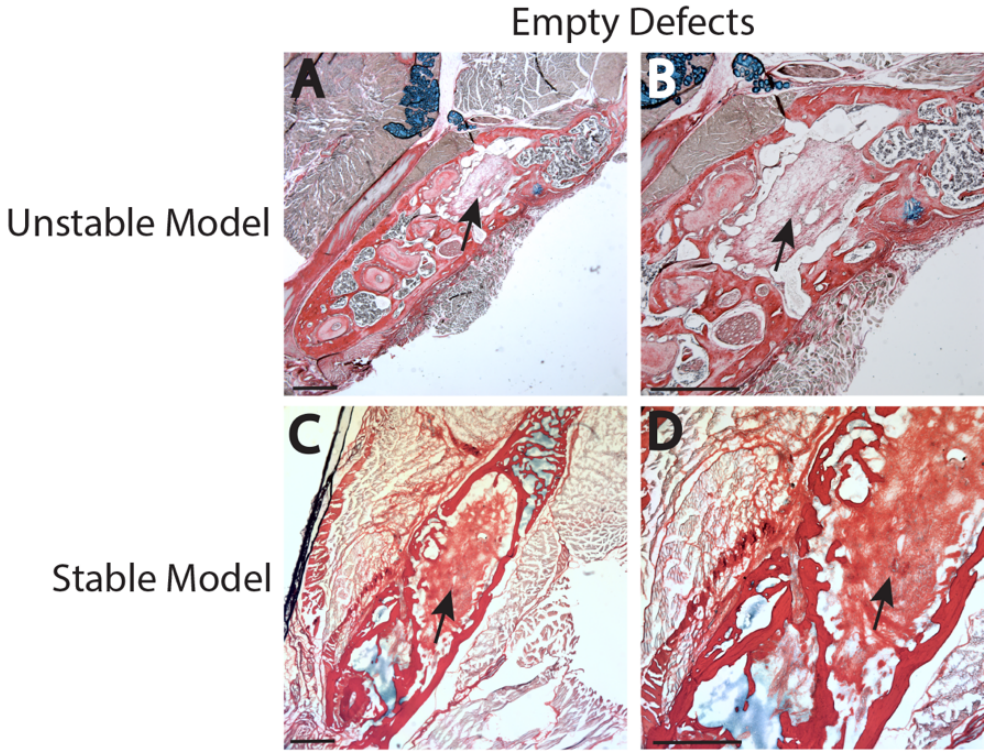

Figure 2.4: Confirmation that Defects are Critical-Sized. Hall Brunt Quadruple/HBQ histology reveals that empty defects, both unstable (A-B) and stable (C-D), are critical-sized. Defects remain unbridged and fill with fibrous tissue (arrows) at 28 days post-fracture, the latest harvest time point. HBQ: cartilage is blue, bone is red. M = Mesial. D = Distal. (*) = Mandibular molar root. Scale=500 μm.

Defects were created in Nude (Nu/J) immunocompromised mice. Graft cartilage was harvested from fracture calli of eGFP or R26 reporter mice 7 days post-fracture and engrafted into defects immediately post-harvest. Mandible samples were harvested 7, 14, and 28 days post-engraftment. HBQ histology revealed that engrafted cartilage began to integrate with the surrounding bone at 7 days post-engraftment, cartilage integration was robust by 14 days post-engraftment, and complete bony-bridging of the defect was observed by 28 days post-engraftment in both models **(Figure 2.5, A-C)**. Newly-formed bone had a robust marrow cavity, indicating healthy and highly-vascularized new bone **(Figure 2.5, C)**. Chondrocytes from the engrafted cartilage as well as osteoblasts and bone-lining cells in the newly-formed bone were X-gal positive, indicating their donor origin **(Figure 2.5, G-I)**. Donor-derived bone (X-gal positive) was clearly distinguished from host-derived bone (X-gal negative) **(Figure 2.5, G).**

DISCUSSION:

Despite several significant differences between craniofacial and long bones, few studies have investigated the fracture repair mechanisms of craniofacial bones. In this study we used mandibular fracture models to identify and compare regulators of repair. Despite differences in embryonic origin and developmental mechanism, mandibular fractures demonstrated similar repair mechanisms as seen in long bones.

One of the basic tenants of long-bone fracture repair is that mechanical motion regulates the mechanism of healing, such that motion promotes cartilage formation and endochondral ossification whereas rigid stabilization results in direct bone formation through intramembranous ossification.[2] In this study we confirm that motion within the mandible plays a similar, dominant role in directing the mechanism of bone formation during fracture repair. Although small regions of cartilage were sometimes observed in our stable fracture samples, it is likely that these pockets

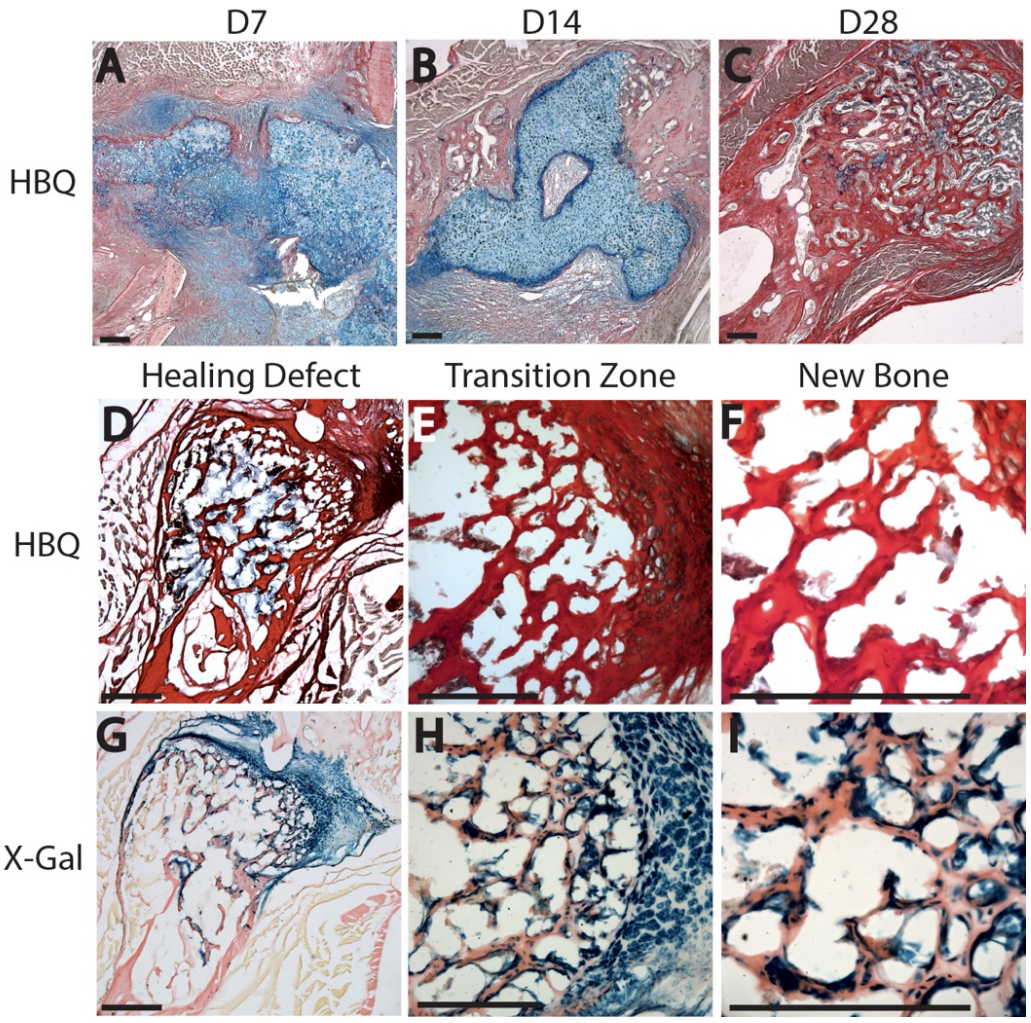

Figure 2.5: Cartilage Engraftment Results in Complete Bony-Bridging of Critical-Sized Mandibular Defects through Graft-Derived Bone Formation. Hall Brunt Quadruple/HBQ shows gradual integration of cartilage grafts with the surrounding bone at 7 (A) and 14 (B) days post-engraftment. Complete bony-bridging of defects occurred by 28 days post-engraftment (C). Newly-formed bone shows a robust marrow cavity, indicating healthy vascularization of the new bone (C). X-gal staining (G-I, corresponds to HBQ in D-F) clearly identifies host versus donor-derived tissues (G) and reveals that osteoblasts and bone-lining cells of the newly formed bone are graft-derived (I). Low magnification images of the defect site (D, G) demonstrate the significant contribution of engrafted cartilage to newly-formed bone, especially at the Transition Zone (E, H). HBQ: cartilage is blue, bone is red. X-gal: donor cells are blue. N=6/time point. Scale=200 μm.

of cartilage formed due to motion created by bone chips that remained post-surgery. Cartilage formation always occurred outside of the trephine defect and was often associated with bone chips. This conclusion is corroborated by tibia fracture studies that show a complete absence of cartilage at all stages of intramembranous repair.[2]

One observation from our study was that stabilized fractures healed faster than those that were unstabilized. Whereas complete bony-bridging was observed in stable fractures at 10 days post-fracture, unstable fractures completely bridged at 21 days post-fracture. The fracture models used in this study differed in both size and shape. Thus, the difference in healing time is likely an artifact of the different fracture designs rather than the result of an intrinsic difference in the rate of healing between endochondral and intramembranous ossification. Indeed, Thompson *et al.* demonstrated using unstabilized versus stabilized transverse tibia fracture models that the time required to achieve bony bridging is identical when bones heal through endochondral versus intramembranous ossification.[2] One limitation of our study is that we did not evaluate the quality of regenerated bone. The degree of bone repair was solely determined by the degree of bone formation and bony bridging through histology.

There has been a centuries-long debate regarding the fate of callus chondrocytes during endochondral repair. In the early 1800's cartilage was believed to transform into bone.[20,77,78] However, in the mid-1800's Muller and Sharpy reported that all chondrocytes ultimately undergo apoptosis and that bone is derived from a separate population of osteoprogenitors.[20] The development of modern murine genetics has enabled accurate lineage tracing and the determination of cell fate. Recent genetic evidence now demonstrates that although some callus chondrocytes undergo apoptosis to make room for the marrow cavity, a significant portion of chondrocytes transform into osteoblasts and directly contribute to the formation of new bone. This has been confirmed using a variety of Cre lines and genetically-labelled transplants in the contexts of long-bone development, growth, and repair as well as mandibular condylar development.[17,22–25,27,79] Here we demonstrated via Aggrecan-Cre^{ERT2} lineage tracing that mandibular callus chondrocytes undergo a similar chondrocyte-to-osteoblast transformation during mandibular fracture repair and that callus chondrocytes significantly contribute to the formation of new bone.

Limited work has been done to investigate the mechanisms that regulate chondrocyte-to-osteoblast transformation. Previous work in long bone fracture repair demonstrates that hypertrophic chondrocytes undergoing chondrocyte-to-osteoblast transformation at the Transition Zone express genes traditionally associated with stem cell pluripotency (*Sox2*, *Oct4*, *Nanog*) as well as classic osteogenic genes (*Runx2*, *Osx*, *OP*, *OC*, *Col1*), suggesting that chondrocytes may undergo stem cell-like plasticity prior to differentiating into osteoblasts.[17,23] Sox2 and β-catenin have been shown to play critical roles in regulating chondrocyte transformation. Hu *et al*. demonstrated that deletion of *Sox2* during repair significantly reduced new bone formation. Houben *et al.* reported similar findings following deletion of β-catenin during endochondral bone development. The presence of nuclear localization of β-catenin in hypertrophic chondrocytes at the Transition Zone indicates that the canonical Wnt pathway may also be involve in regulating chondrocyte transformation during endochondral repair.[17]

In this study we looked to understand if phenotypic modulation of mandibular chondrocytes paralleled that seen in long bone fracture repair. Evidence presented here suggests further similarity in the regulatory mechanisms of craniofacial and appendicular bones during fracture repair. The Transition Zone histomorphometry of mandibular fractures was similar to that seen in previously-published tibia fracture studies.[17,22,23,25,27] Furthermore, mandibular chondrocyte gene expression in the hypertrophic region at the Transition Zone paralleled that seen previously in tibial fracture studies, with chondrocytes expressing the stem cell marker Sox2 and osteogenic gene osteocalcin (*OC*). It is important to note that expression of these proteins is limited almost exclusively to hypertrophic chondrocytes located at the Transition Zone and that expression is absent or significantly lower in pre-hypertrophic chondrocytes.

Since cartilage transforms into bone in an endogenous healing context, there has been increasing interest in the development of cartilage-based therapies. Bahney *et al.* demonstrated that cartilage grafts heal critical-sized tibial defects and that a significant portion of newly-formed bone is donor-derived.[23] Furthermore, they demonstrated that human bone marrow-derived mesenchymal stem cells (hMSCs) can be differentiated and cultured into viable cartilage grafts for transplant.[23] Other studies have also demonstrated the efficacy of using cartilage to engineer bone. Scotti *et al.* demonstrated that subcutaneous implantation of hypertrophic cartilage derived from hMSCs gives rise to an ectopic "bone organ" with a structure and functionality comparable to that of native bones.[70] Dang *et al.* reported that critical-sized calvarial defects can heal through endochondral ossification when treated with hMSCs pushed towards chondrogenesis through the controlled release of transforming growth factor-beta 1 (TGF-β1) and bone morphogenetic protein-2 (BMP-2) delivered via bioactive microparticles.[67] And Cunniffee *et al.* showed that decellularized hypertrophic cartilage freeze-dried to generate porous scaffolds can produce complete bony bridging of critical-sized femoral defects.[80]

Our data support that cartilage is an effective tissue graft to promote bone regeneration in the mandible in both stabilized and unstabilized fracture contexts. Thus, the ability of cartilage to heal critical-sized defects is not limited by the endogenous healing pathway and is effective for vascular bone regeneration. Importantly, since complete mandibular healing was attained through the use of tibia-derived cartilage, our data indicates that the embryonic origin or mode of tissue development does not significantly impact the efficacy of graft tissues.

Autologous bone grafts are the current gold standard of care. In the case of mandibular reconstruction, non-vascularized grafts are traditionally harvested from the rib or iliac crest, whereas vascularized free flaps are primarily harvested from the fibula.[81] Due to the necessity of the vasculature for graft survival, non-vascularized bone grafts are only used to treat small defects

where a robust vascularized tissue bed is already present. A flap is required in cases of soft tissue injury.[81] Although autologous bone grafts have had significant clinical success, they require a second surgical site, are often accompanied by donor site morbidity, and have limited supply.[23,28] Bone allografts have been developed as an alternative graft material and are readily available; however, they have significantly reduced bioactivity and a high rate of clinical failure due to poor osteointegration and osteonecrosis of the graft.[29] Unlike bone, cartilage is an avascular tissue that is not only capable of surviving without a vascular supply but is also responsible for recruiting blood vessel invasion for the newly-formed bone during endochondral ossification.[1,82] Thus, cartilage is not only better suited to survive within poorly vascularized areas of tissue injury but its use also parallels the natural healing process of endochondral repair. The data presented here provide promising evidence in support of using cartilage as an alternative graft tissue.

CONCLUSION:

Although craniofacial bones and long bones have significant developmental differences, our study provides direct evidence demonstrating that these bones heal via similar mechanisms. Notably, during endochondral fracture repair, both sets of bones rely on the significant contribution of chondrocytes for the formation of new bone through chondrocyte-to-osteoblast transformation. This data provides important insight into the enhancement of craniofacial fracture therapies, such as the use of cartilage as a graft tissue, and it supports the application of findings from appendicular fracture studies to the treatment of craniofacial fractures.

Chapter 3:

Porcupine-Independent Wnt/β-catenin Signaling is Required for Chondrocyte-to-Osteoblast Transformation during Endochondral Repair

The majority of fractures heal through the process of endochondral ossification, in which a cartilage intermediate forms between the fractured bone ends and is gradually replaced with bone.[82–84] This process begins with the differentiation of progenitor cells primarily derived from the periosteum into chondrocytes, which proliferate to form the cartilage callus.[3,4] As chondrocytes mature to a hypertrophic state, they mineralize their surrounding matrix and promote vascular invasion.[15,17,59,60,85] Genetic lineage tracing studies demonstrate that hypertrophic chondrocytes directly contribute to the formation of bone by transforming into osteoblasts.[17,22–24,79,86,87] This transformation has been confirmed using a variety of genetic models during bone development, postnatal growth, and repair in the appendicular and craniofacial skeletons.[17,22–24,79,86,87] However, little is known regarding the molecular signals that regulate this process during bone healing.[17,24]

Canonical Wnt signaling may play a key role in regulating chondrocyte-to-osteoblast transformation during endochondral repair. Loss-of-function and gain-of-function experiments modifying this pathway in chondrocytes have demonstrated the necessity of this pathway to chondrocyte transformation during long-bone development.[24] In the context of endochondral repair, hypertrophic chondrocytes located at the chondro-osseous border of the fracture callus, where chondrocyte-to-osteoblast transformation occurs, have been shown to have nuclear localization of β-catenin, indicating that these cells undergo active canonical Wnt signaling.[17]

Canonical Wnt signaling requires the co-activator β-catenin to mediate its effect in modulating gene expression.[42,84] β-catenin is constitutively expressed. However, when the pathway is inactive, β-catenin is targeted for ubiquitin-mediated degradation by a multi-protein “destruction

complex." When the canonical Wnt pathway is activated through the binding of Wnt ligands to Frizzled and LRP5/6 receptors, the destruction complex is disrupted, stabilizing β-catenin in the cytoplasm and allowing it to translocate to the nucleus where it binds to members of the T-cell factor/lymphocyte elongation factor (TCF/LEF) family to regulate Wnt target gene expression.[42,84]

The canonical Wnt pathway is predominantly activated by Wnt ligands. However, ligand-independent activation of the pathway has been noted in numerous biological contexts.[88–110] Wnts are hydrophobic due to the addition of palmitate and/or palmitoleic acid to cystine and serine residues.[56,57] This acylation has been shown to be required for Wnt intracellular trafficking, secretion, and for full biological activity.[55,56] Genetic evidence indicates that the O-acyltransferase Porcupine is required for Wnt palmitoylation as well as intracellular transport of Wnts from the endoplasmic reticulum for secretion.[56,111–113] Hence, deletion of Porcupine results in a significant reduction in Wnt pathway activation via Wnt ligands.

Due to the Wnt pathway's established role in promoting bone formation, numerous Wnt-based therapies are currently being developed.[82] The hydrophobic nature of Wnt ligands and the requirement of palmitoylation for biological activity precludes treatment with recombinant Wnts as a clinical therapeutic.[55–58,82] Thus, the majority of Wnt-based therapies aim to activate the Wnt pathway by neutralizing pathway inhibitors, such as Dkk1 and sclerostin.[54,82] One promising Wnt pathway regulator, Romosozumab, is a monoclonal antibody that works by binding and inhibiting the activity of sclerostin.[52,54,82] Romosozumab received FDA approval in April 2019 for treatment of osteoporosis. Understanding endogenous Wnt signaling during endochondral fracture repair is critical to optimizing the timing and cellular targets of Wnt therapeutics for bone regeneration.

In this paper we demonstrate that activation of canonical Wnt signaling during chondrocyte-to-osteoblast transformation is necessary for normal fracture repair. We also demonstrate that

although numerous callus tissues express Wnts, pathway activation is independent of Porcupine-mediated Wnt modification, suggesting that Wnt ligands likely play a minor role in activating chondrocyte canonical Wnt signaling. This evidence provides key insight into the process of endochondral repair and advances the development of novel Wnt-based fracture therapies.

MATERIALS AND METHODS:

Fractures

All studies were approved by the UCSF Institutional Animal Care and Use Committee. The following mice were obtained from Jackson Labs: Aggrecan-Cre^{ERT2} (Stock #: 019148), β-Catenin floxed (Stock #: 004152), tdTomato HZE (Stock #: 007909), R26-Cre^{ERT2} (Stock #: 008463), and C57BL/6J (Stock #: 000664). Cttnb1GOF,[114] Cdh5(PAC)-CreERT2,[115] and Porcupine floxed mice (Jackson Stock #: 020994) were obtained with MTA approval (if applicable) from our collaborators at UCSF and maintained in our colony for the duration of this study. Genotype was confirmed for all mice through gel electrophoresis according to Jackson labs and donor lab's genotyping protocols. Adult (10-18 week) male mice were anesthetized with a 1:1 mixture of ketamine (60 mg/kg) and dexmedetomidine (0.3 mg/kg). Closed non-stable fractures were created in the mid-diaphysis of the right tibia through 3-point bending.[116] Fractures were not stabilized to promote robust endochondral repair. Animals were revived using an atipamezole reversal agent (6 mg/kg) and were given buprenorphine analgesic (0.05-0.1 mg/kg) immediately post-op, at 4 and 24 hours post-fracture, and as needed. Cre recombination was induced with daily injections of Tamoxifen (75 mg/kg in corn oil, Sigma, #T5648-5G) from days 6 to 10 post-fracture.[17] Mice were monitored and allowed to ambulate freely until harvest at 7, 10, 14, and 21 days post-fracture (N>5/group/time point). To identify any potential differences in fracture repair based on sex, female mice were also harvested at 14 days post-fracture (N>5/group).

Histology

Fractured tibiae were fixed in 4% paraformaldehyde (PFA, pH 7.4) for up to 24 hours at 4C and decalcified for 2 weeks in 19% ethylenediaminetetraacetic acid (EDTA, pH 7.4). EDTA was replenished 5 times per week. Tibiae were either paraffin or cryo-embedded. Tissues were sectioned (10 μm) for histological and fluorescence analysis. Halls Brunt Quadruple (HBQ) histology was used to visualize cartilage and bone (cartilage stains blue, bone stains red). N>5/group/time point.

Stereology

Quantification of callus size and composition (cartilage, bone, fibrous, marrow space) was determined using an Olympus CAST system (Center Valley, PA) and software by Visiopharm (Hørsholm, Denmark) according to established methodologies.[117] HBQ stained serial sections through the entire leg, spaced 300 μm apart were analyzed. The fracture callus was outlined using low magnification (20x, 2X objective with 10X ocular magnification) to determine the region of interest. 7-15% of this region was quantified using automated uniform random sampling to meet or exceed the basic principles of stereology.[117] Cell and tissue identity within each random sampling domain was determined at high magnification (200X, 20X objective with 10X ocular magnification) according to histological staining patterns and cell morphology. Absolute volumes of specific tissues (e.g. bone or cartilage) were determined using the Cavalieri formula and these absolute volumes were used to determine the relative percent composition of tissues within the fracture callus.[117] Total fracture callus volume was measured as callus points. Marrow space was identified as tissue that fell within a blood vessel or marrow cavity of the new bone.

TUNEL Assay

The Roche In Situ Cell Death Detection Kit (Roach, #11687959) was used according to the manufacturer's protocol. Sections were deparaffinized, treated with proteinase K (20 ug/ml in 10

mM Tris-HCl, pH 8, 15 min), and then reacted with the kit for 1 hour at 37C in the dark. Positive controls were treated with DNase I prior to TUNEL reaction, while negative controls were not treated with the TUNEL reaction enzyme. Slides were mounted in VectaShield with DAPI (Vector, #H-1200) and visualized using an epifluorescence microscope (Leica DM500B).

Lineage Tracing

Aggrecan-Cre$^{ERT2/+}$::β-catenin$^{fl/fl}$::tdTomatoHZE$^{/+}$ mice were used to assess chondrocytes following deletion of β-catenin, and Cdh5(PAC)-Cre$^{ERT2/+}$::tdTomatoHZE$^{/+}$ mice were used to confirm Cre specificity to endothelial cells. Unstable fractures were created and tamoxifen was administered as above. Samples were harvested 14 days post-fracture, fixed and decalcified as above, cryoembedded, and sectioned (10 μm). Samples were mounted in VectaShield with DAPI (Vector, #H-1200) and visualized using an epifluorescence microscope. N=3/genotype.

Immunohistochemistry

Immunohistochemistry for PECAM (BD Pharmingen, #553370, 1:100) was performed on cryo-embedded sections of tibiae harvested 14 days post-fracture (N>3). Immunohistochemistry for F4/80 (eBiosciences, #144801, 1:100) was performed on paraffin-embedded sections of tibiae harvested 10 days post-fracture (N>3). The basic protocol for both antibodies included endogenous peroxidase blocking in 3% H_2O_2 (30 min, RT), antigen retrieval in 0.1% Trypsin (20 min at 37C then 20 min at RT), and non-specific epitope blocking with 5% goat serum (1 hr, RT). Primary antibodies were applied to sections overnight at 4C. Biotinylated species-specific secondary antibodies were diluted in PBS with 5% GS and applied to tissues for 1 hr at room temperature (Pecam: BD Pharmingen, #559286, 1:250. F4/80: Santa Cruz, #sc-2041, 1:250). Staining was detected using the VectaStain ABC Elite Kit (#PK-6100) and 3,3'-diaminobenzidine (DAB) colorimetric reaction.

TRAP Staining

TRAP staining was performed on paraffin sections using the Sigma TRAP staining kit (#387A) according to the manufacturer's protocol. Slides were mounted with Permount and visualized with brightfield or DIC microscopy.

HUVEC Conditioned Media

Human umbilical vein endothelial cells (HUVECs) were cultured in Medium 200 (Gibco, #M-200-500) with Large Vessel Endothelial Supplement (LVES 50X, GIBCO, #A14608-01), 1% Penicillin/Streptomycin, and 10% MSC FBS (Gibco, #12662-029) until ~70% confluent. Cells were washed twice with dPBS and cultured for an additional 48 hours without FBS. Conditioned media was filtered (0.22μm) and stored at -80C. HUVECs were harvested into TRIzol (Invitrogen, #15596026) and stored at -80C. N=11 media harvests.

Wnt Reporter Assay

293-STF luciferase Wnt reporter cells were obtained from the Christopher Garcia laboratory.[118] Cells were seeded at 20,000 cells/well in a 96-well plate and cultured overnight in DMEM (Gibco, #10566-016), 10% FBS, 1% Pen/Strep. Cells were treated with 20% HUVEC-conditioned media (HUVEC-CM), 2 nM Wnt3a, or with unconditioned media for 24 hours. All samples were run in technical triplicates and received 25 nM Rspon2-Fc. The Dual-Luciferase Reporter Assay System (Promega, #E1960) was used to assess luciferase activity.

RT-PCR

Fracture calli were harvested 10 days post-fracture from β-catenin gain-of-function and control mice in order to assess Axin2 gene expression and confirm over-activation of the canonical Wnt pathway. Callus tissues were isolated from surrounding muscle and cortical bone and homogenized in TRIzol (Invitrogen, #15596026). RNA isolation was performed according to the

manufacturer's protocol followed by DNase treatment (Invitrogen, #Am1906). cDNA was reverse transcribed with iScript cDNA Synthesis Kit (Bio-Rad, #1708890) and quantitative RT-PCR was performed using SYBR-based primers (**Table 3.1)** and RT SYBR Green qPCR Mastermix (Qiagen, #330509) on a CFX96 Touch Thermal Cycler (Bio-Rad) run to 50 cycles (N=3-5/treatment group). RNA isolation, DNase treatment, and reverse transcription was performed as above for Wnt expression analysis on HUVEC cells. However, TaqMan probes **(Table 3.2)** and TaqMan Universal Master Mix II with UNG (#4440038) were used. Analysis was run on a CFX96 Touch Thermal Cycler (Bio-Rad) to 45 cycles (N=3). All samples were run in triplicate and relative gene expression was calculated by normalizing to the housekeeping gene GAPDH ($2^{-\Delta CT}$). Fold change was calculated as $2^{-\Delta\Delta CT}$.

FACS

Macrophages (CD45+, F4/80+, CD11b+), endothelial cells (CD31+, Ve-Cadherin+), and total callus CD45+ and CD45- cell populations were isolated from C57BL/6 mice at 14 days post-fracture, whereas chondrocytes (tdTomato+, CD45-) were isolated from Aggrecan-CreERT2$^{/+}$::tdTomato HZE$^{/+}$ reporter mice at post-fracture day 10 after tamoxifen injection from days 6-10. A defined area around the fracture callus was isolated, weighed, skin and muscle eliminated and bone marrow discarded or stored separately. The remainder of the fracture callus was minced and disassociated manually in Collagenase/Dispase (1 µg/ml, Roche, #10269638001) followed by digestion for 1 hour at 37 degrees. After digestion the cells were passed through a 100µm filter and rinsed with PBS. Cells were then pelleted and counted with a hemocytometer. Isolated cells were blocked for 10 minutes at room temperature with anti-FcR antibodies (ATCC, 24G2 hybridoma) and then stained directly with conjugated fluorescent antibodies **(Table 3.3)**. Red Dead or Ghost Violet (Biosciences, #13-0863-T100) was used for the detection of dead cells. Isotype controls and fluorescence minus one controls were used to gate

for background staining. Cells were sorted on a FACSAriaIII (BD Biosciences, San Jose, CA) and FlowJo Software 9.6 (Treestar, Ashland, OR) was used for analysis. N=3/population.

Fluidigm Gene Expression Analysis

Total RNA was isolated from FACS-sorted cells using the Arcturus PicoPure RNA Isolation Kit (Thermo, #12204-01) and was DNase treated (Ambion DNA-Free: DNase Treatment & Removal Kit, #AM1906) according to the manufacturer's protocols. RNA was reverse transcribed into cDNA using Maxima H Minus Reverse Transcriptase (Thermo, #EP0752) followed by RNase treatment with RNAse H (Thermo, #18021071). Pre-amplification of cDNA was performed using the Fluidigm Pre-Amp MasterMix (Fluidigm, #100) and TaqMan assays **(Table 3.2)** according to manufacturer's instructions. qPCR for GAPDH and β-actin was performed in technical triplicates for all samples using a Viia7 thermocycler (Invitrogen) to determine optimal cDNA sample concentration. Complete gene expression analysis was performed for all samples using a BioMark 48.48 dynamic array nanofluidic chip (Fluidigm Inc., BMK-M-48.48, #68000088). Ct values were normalized to the housekeeping gene GAPDH. N=3/cell population.

Cre Recombination Efficiency

Callus tissues were isolated from 6-12 paraffin sections on slides adjacent to those used for stereological quantification. The callus region was carefully traced and surrounding extraneous tissue removed prior to harvest of the callus and incubation of tissue in 100µl lysis buffer (1M Tris HCl pH 8.0, 0.5M EDTA pH 8.0, 10% SDS, 5M NaCl) with 3.33µl Proteinase K (10mg/mL) for 3 hours at 55C. DNA isolation was performed using isopropanol precipitation, followed by a 70% EtOH wash and resuspension in H_2O. The DNA concentration of all samples was adjusted to 5.5 ng/µl. SYBR green qPCR was subsequently performed using 11ng of DNA per well and primers designed by Liu *et al.* to recognize wildtype, floxed, and floxed-deleted Porcupine alleles.[119] P1-P2 and P3-P4 primer pairs recognize wildtype and floxed sequences, whereas the P1-P4 primer

pair only amplifies the floxed-deleted allele. C_T values were normalized to the housekeeping gene Techtonic 3 and to the corresponding experimental control. N=5/group.

Statistics

Data plots were generated using GraphPad Prism 8. Initial analysis of variance was assessed using RStudio and statistical significance was determined with Prism. The non-parametric Mann-Whitney-Wilcoxon test was used when comparing two groups. ANOVA followed by post-hoc multiple-comparisons analysis through Tukey's HSD test was used when comparing more than two groups. $P \leq 0.05$ was designated as statistically significant.

RESULTS:

Inhibition of Canonical Wnt Signaling in Fracture Callus Chondrocytes Significantly Reduces Bone Formation During Repair:

To determine the role of canonical Wnt signaling in regulating chondrocyte-to-osteoblast transformation, the pathway was conditionally inhibited in chondrocytes by inducing deletion of β-catenin using the Aggrecan-Cre^{ERT2} mouse. Cre recombination was induced with daily injections of Tamoxifen from 6 to 10 days post-fracture, which has been previously shown to induce robust Cre recombination in chondrocytes.[17,86] Cartilage formation at early stages of repair was unaffected (D7 & D10). However, significantly reduced bone formation and increased cartilage retention occurred at later time points (D14 & D21) during which chondrocyte transformation primarily occurs **(Figure 3.1)**. A statistically significant reduction in bone formation was observed with deletion of either one or both copies of β-catenin. However, the reduction in bone formation was greater with the loss of both copies. **(Figure 3.2)**.

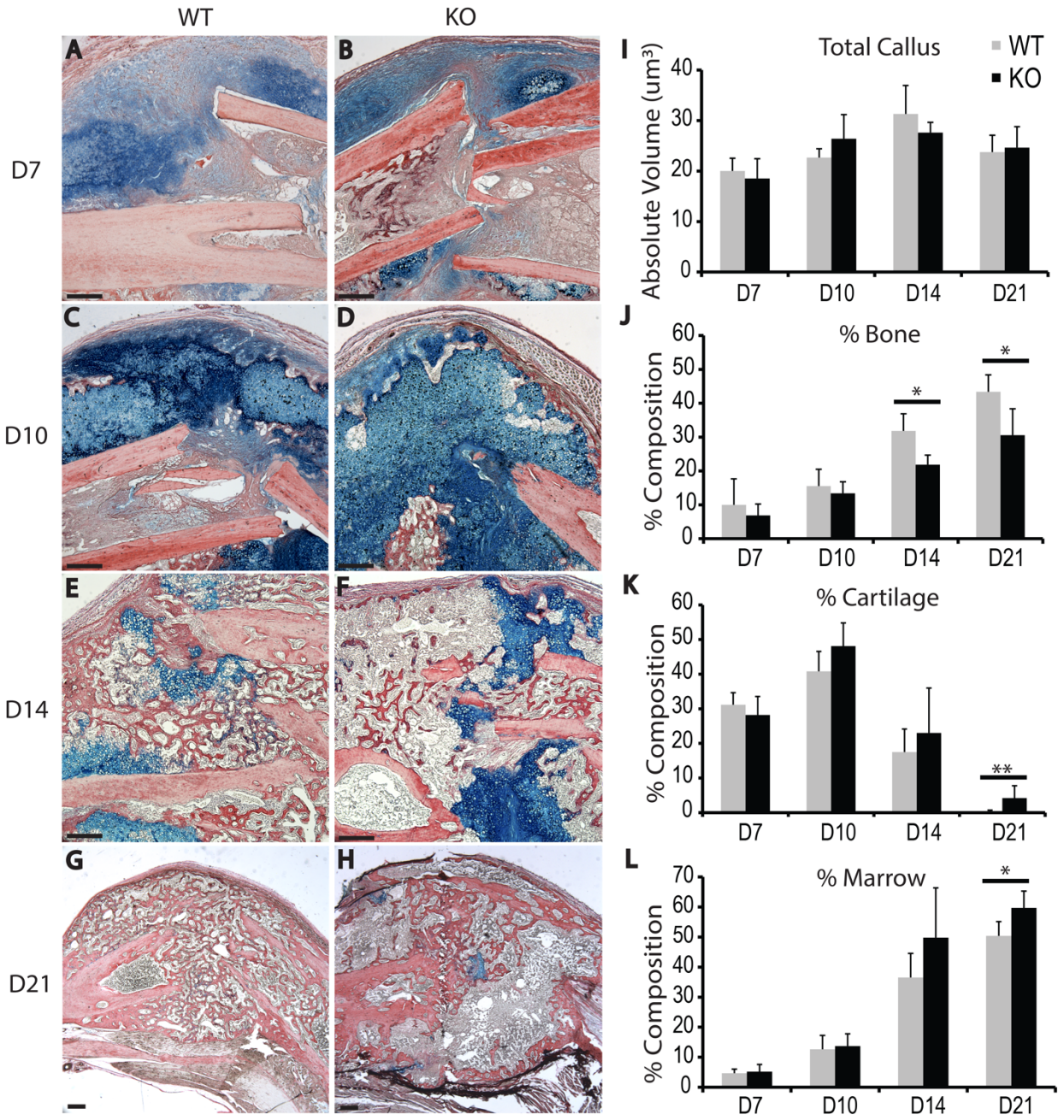

Figure 3.1: Deletion of β-catenin in Chondrocytes Significantly Impairs Endochondral Healing. Stereological quantification (I-L) of HBQ histology (A-H) reveals that inhibition of canonical Wnt signaling through conditional deletion of β-catenin in chondrocytes significantly reduces trabecular bone formation (E-H, J) and increases cartilage retention (G-H, K) at later time points (D14, D21). Callus size and composition are unaffected at early time points (D7, D10). HBQ histology: cartilage = blue, bone = red. N=5/group/time point. Scale bar = 1000μm. (*) = $p < 0.05$. (**) = $p < 0.01$.

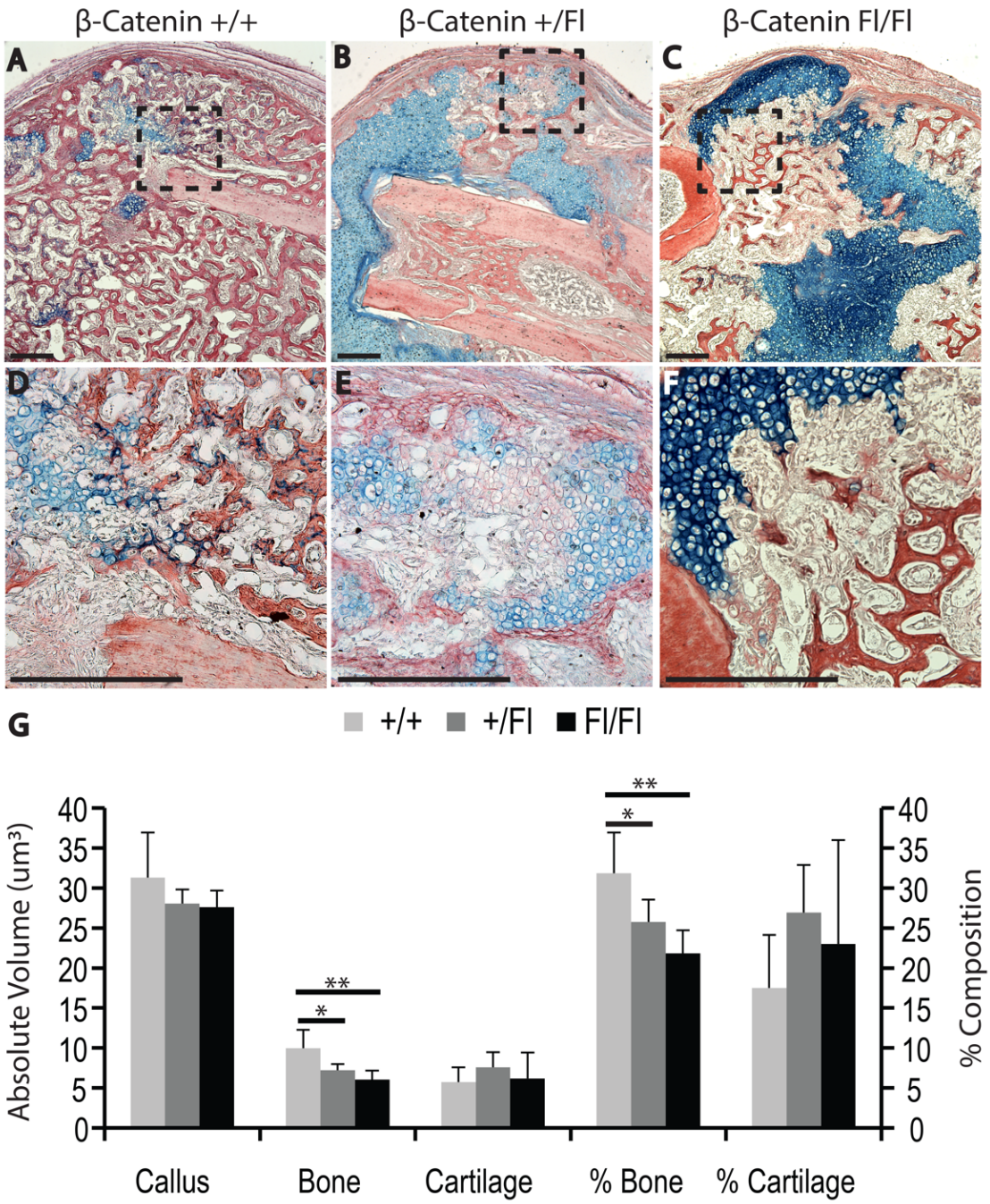

Figure 3.2: Statistically Significant Reduction in Bone Formation Results from Deletion of Either One or Both Copies of β-catenin in Chondrocytes. Stereological quantification (G) of HBQ histology (A-F) reveals that inhibition of canonical Wnt signaling through conditional deletion of either one (B,E) or both (C,F) copies of β-catenin in chondrocytes results in a statistically significant reduction in absolute bone volume and % bone composition. A greater reduction is observed with the loss of both copies. HBQ histology: cartilage = blue, bone = red. N=5/group/time point. Scale = 1000μm. (*) = p< 0.05. (**) = p< 0.01.

The above experiments were conducted using male mice. To confirm that the canonical Wnt pathway plays a similar role in female mice, females were harvested at 14 days post-fracture. Analysis revealed that deletion of β-catenin in chondrocytes of female mice produced a similar reduction in bone formation and increase in cartilage retention **(Fig 3.3, A)** as seen in male mice **(Figure 3.1, E-F, J-K)**. Furthermore, comparison of male and female mice revealed that although females had significantly lower body weight than males **(Figure 3.3, B)**, there was no statistically significant difference between sexes for tissue composition parameters when normalized to body weight **(Figure 3.3, C-D)**, except for a slight increase in total callus size in females when β-catenin was deleted **(Figure 3.3, C).**

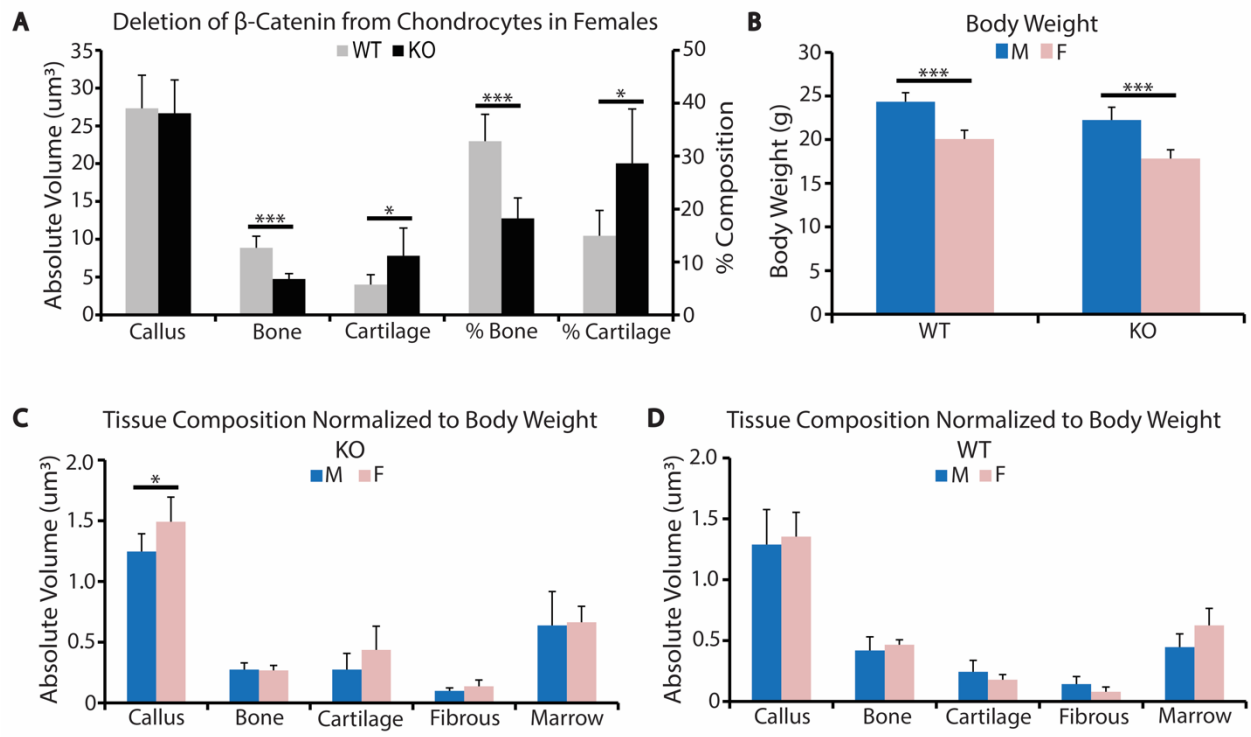

Figure 3.3: Canonical Wnt Signaling Regulates Chondrocyte-to-Osteoblast Transformation in Both Males and Females. Stereological analysis of fractures harvested from female mice at 14 days post-fracture reveals that inhibition of canonical Wnt signaling in chondrocytes through deletion of β-catenin significantly reduces bone formation and increases cartilage retention compared to controls (A). Although female mice have a significantly lower body weight compared to male mice (B), there is no statistically significant difference in tissue composition between sexes for control mice when normalized to body weight (D). There is a slight increase in total callus size in female mice compared to males when β-catenin is deleted (C). However, all other tissue parameters show no statistically significant difference. N=5/group/time point. (*) = $p < 0.05$. (***) = $p < 0.001$.

TUNEL staining revealed that deletion of β-catenin did not significantly increase chondrocyte cell death. Indeed, lineage tracing analysis using a tdTomato reporter showed survival of chondrocytes as detached cells filling the marrow space **(Figure 3.4)**. tdTomato-positive cells were observed within the marrow cavity as late as 35 days post-fracture (data not shown). The specificity of tdTomato fluorescence was confirmed by complete absence of expression in marrow cells found at the growth plate of reporter mice **(Figure 3.4, E, H)**. Furthermore, no tdTomato expression was observed in chondrocytes or marrow cells of fracture calli from mice lacking the tdTomato reporter **(Figure 3.4, F, I)**.

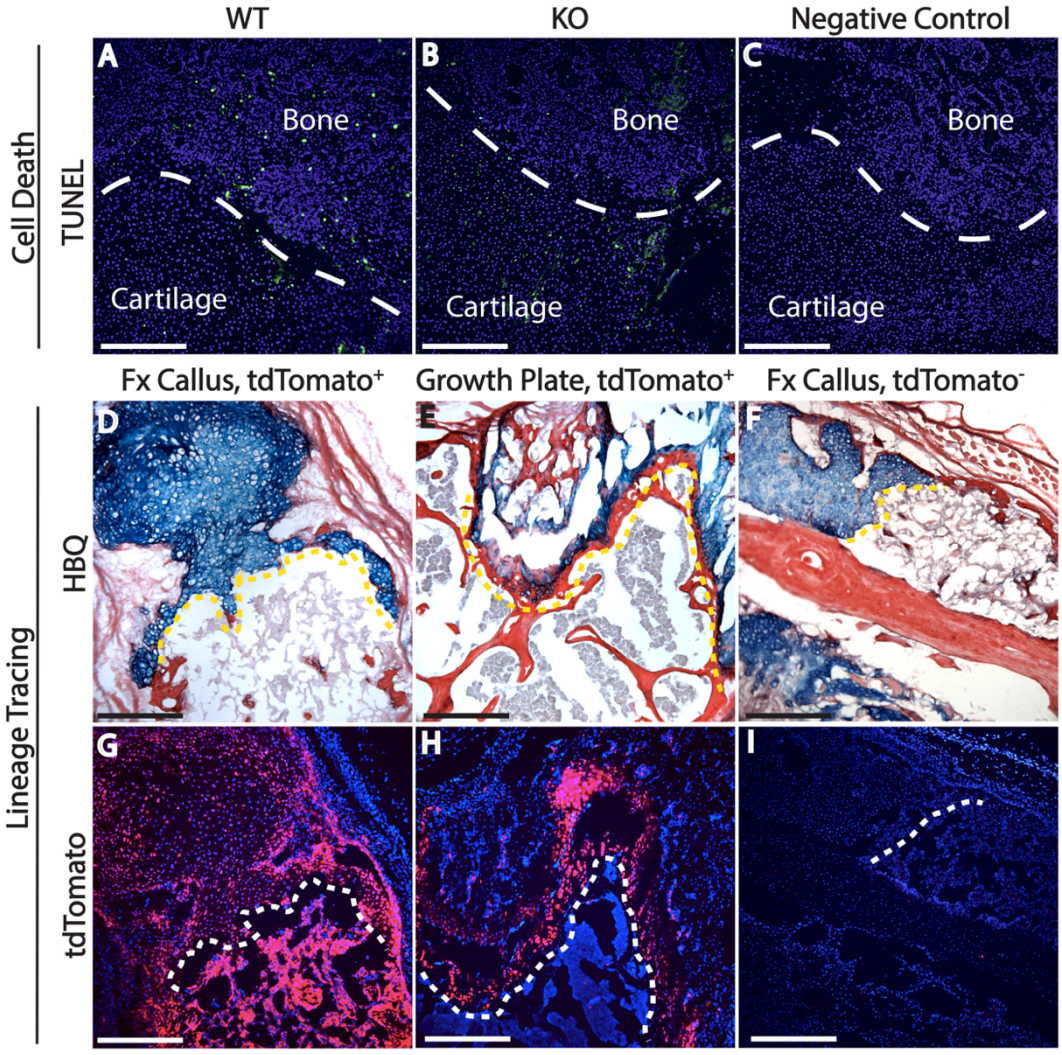

Figure 3.4: Chondrocytes Survive within the Marrow Cavity Following Deletion of β-catenin
TUNEL analysis (A-C) at 14 days post-fracture demonstrates that inhibition of canonical Wnt signaling in chondrocytes through deletion of β-catenin does not significantly increase

chondrocyte cell death. Furthermore, lineage tracing analysis (D-I) using a tdTomato reporter at 14 days post-fracture reveals that chondrocytes survive within the marrow cavity following deletion of β-catenin. The specificity of tdTomato fluorescence was confirmed by its complete absence in marrow cavity cells found at the growth plate of reporter mice (E, H) as well as in chondrocytes and marrow cells of fracture calli from wildtype mice lacking the tdTomato reporter (F, I). HBQ histology (D-F): cartilage = blue, bone = red. DAPI counterstain was used to visualize nuclei, (A-C, G-I, blue). N=5. Scale = 200μm.

Loss of β-catenin resulted in unique changes to Transition Zone morphology. Unlike controls, callus cartilage did not directly connect to trabecular bone. Rather, callus chondrocytes appeared to “slough off” into the marrow space, a process potentially aided by TRAP-positive cells, which exhibited increased localization to the borders of the cartilage callus **(Figure 3.5)**.

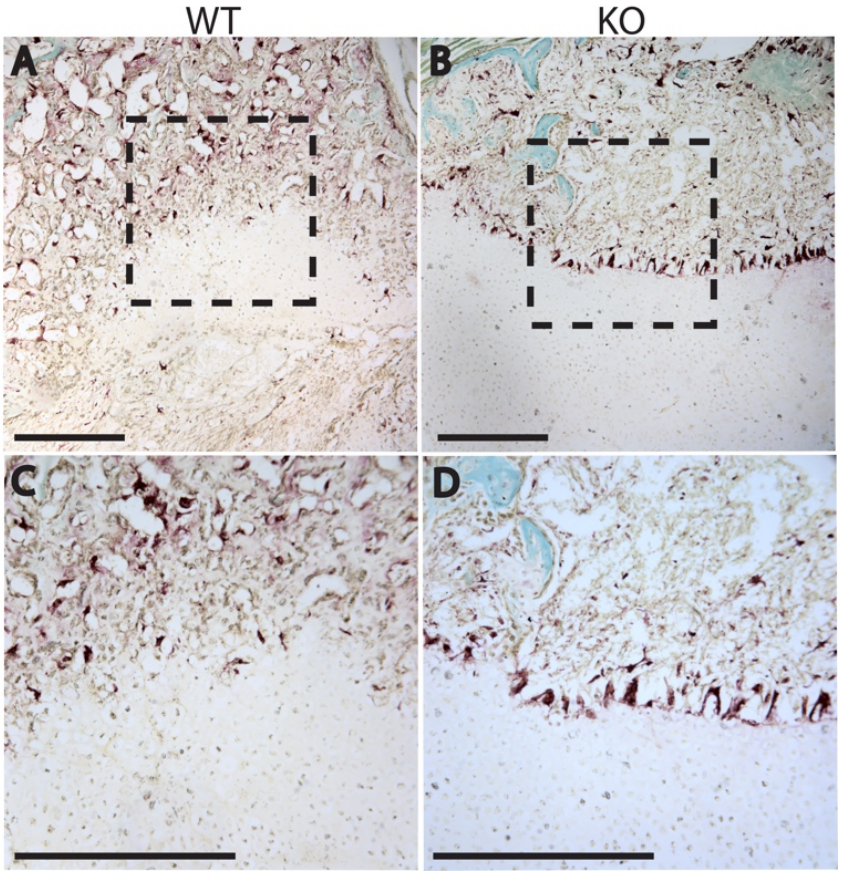

Figure 3.5: TRAP Staining Reveals Increased Localization of Osteoclasts to the border of the Cartilage Callus after Deletion of β-catenin in Chondrocytes. TRAP staining (A-D) reveals increased localization of osteoclasts at the cartilage callus border following deletion of β-catenin in chondrocytes (B,D) compared to controls (A,C). Fast Green counter stain. N=5. Scale = 200μm.

Interestingly, a significant population of FACS-analyzed tdTomato+ marrow cells was positive for CD45, a marker of hematopoietic cell lineages **(Figure 3.6, B)**.[120,121] In contrast, marrow cells from control mice expressing the tdTomato reporter but possessing wildtype copies of β-catenin demonstrated neither significant tdTomato fluorescence nor significant tdTomato, CD45 dual-labelling **(Figure 3.6, C)**. CD45 staining did not bleed into the tomato channel as evidenced by minimal CD45 staining observed in unstained cells **(Figure 3.6, A, D).** Furthermore, the degree of tdTomato, CD45 dual-labelling in control mice **(Figure 3.6, C;** β-catenin+/+, tdTomato+**)** was comparable to that seen in wildtype mice **(Figure 3.6, F;** β-catenin+/+, tdTomato-**)**, which did not possess the tdTomato reporter. Together this data indicate that callus chondrocytes do not, under normal conditions, remain detached within the marrow cavity and that deletion of β-catenin in chondrocytes promotes their engulfment by hematopoietic cells.

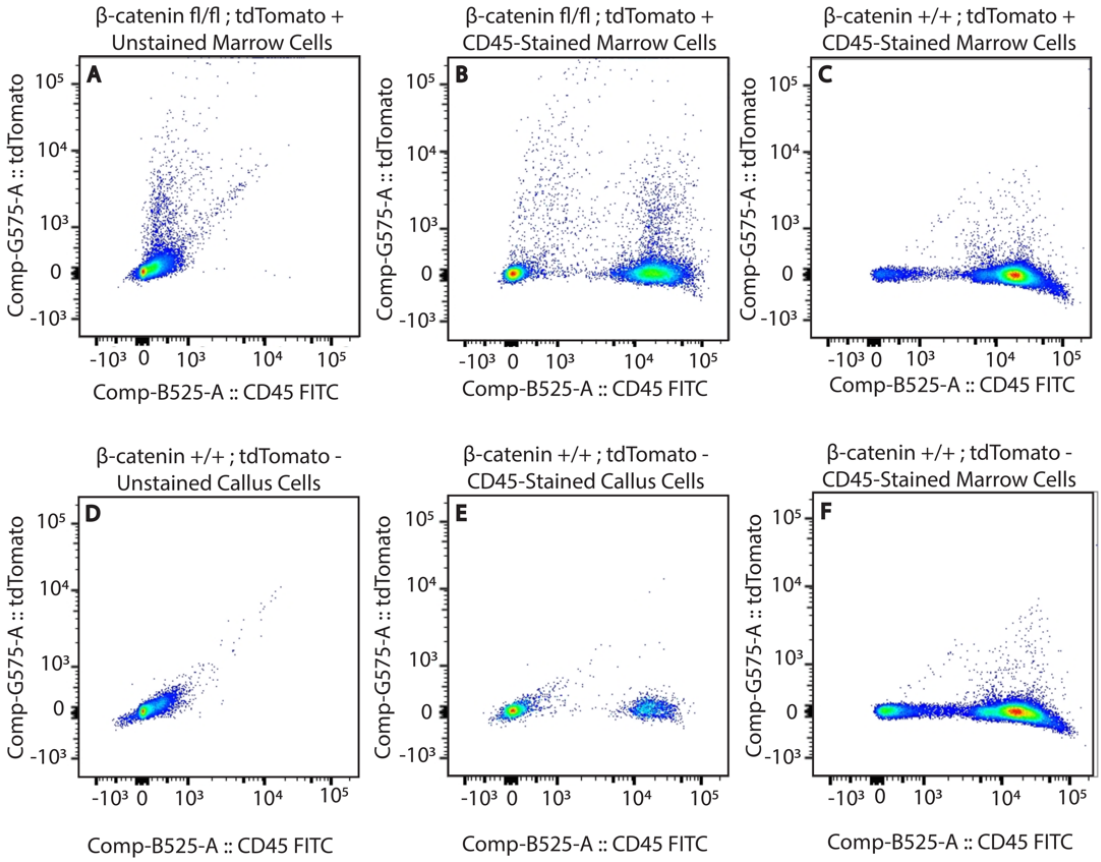

Figure 3.6: FACS Analysis of tdTomato+ Cells Reveals Chondrocyte Engulfment by Phagocytic Hematopoietic Cells. FACS analysis reveals that deletion of β-catenin results in a significant population of tdTomato+ marrow cells that are also positive for CD45 (B). In contrast, FACS-

analysis of marrow cells from control mice (β-catenin +/+, tdTomato+) demonstrates neither significant tdTomato+ fluorescence nor significant tdTomato+, CD45+ dual-labelling (C). CD45 staining did not bleed into the tomato channel as evidenced by minimal CD45 staining observed in unstained cells (A, D). Furthermore, the degree of tdTomato, CD45 dual-labelling in control mice (C; β-catenin+/+, tdTomato+) was comparable to that seen in wildtype mice (Fig 3, F; β-catenin+/+, tdTomato-). Together this data indicate that callus chondrocytes do not, under normal conditions, remain detached within the marrow cavity and that deletion of β-catenin in chondrocytes promotes their engulfment by hematopoietic cells. N=3/cell population.

Over-activation of Canonical Wnt Signaling in Fracture Callus Chondrocytes Accelerates Bone Repair by Promoting Chondrocyte Transformation:

The converse, gain-of-function experiment was performed in which an indestructible, stabilized form of β-catenin was induced to be conditionally expressed in chondrocytes starting six days post-fracture. RT-PCR analysis of Wnt target gene *Axin2* expression in fracture calli harvested 10 days post-fracture confirmed that canonical Wnt signaling was over-activated **(Figure 3.7, M)**. Wnt pathway gain-of-function not only increased the absolute volume and percent callus composition of bone compared to controls, but it also accelerated bone formation as evidenced by the shift in bone formation to earlier time points (D10) **(Figure 3.7, O)**. This increase in bone formation corresponded with a simultaneous significant reduction in callus cartilage composition **(Figure 3.7, P)**. Together, these data suggest that stimulation of canonical Wnt signaling in chondrocytes results in accelerated chondrocyte-to-osteoblast conversion **(Figure 3.7)**.

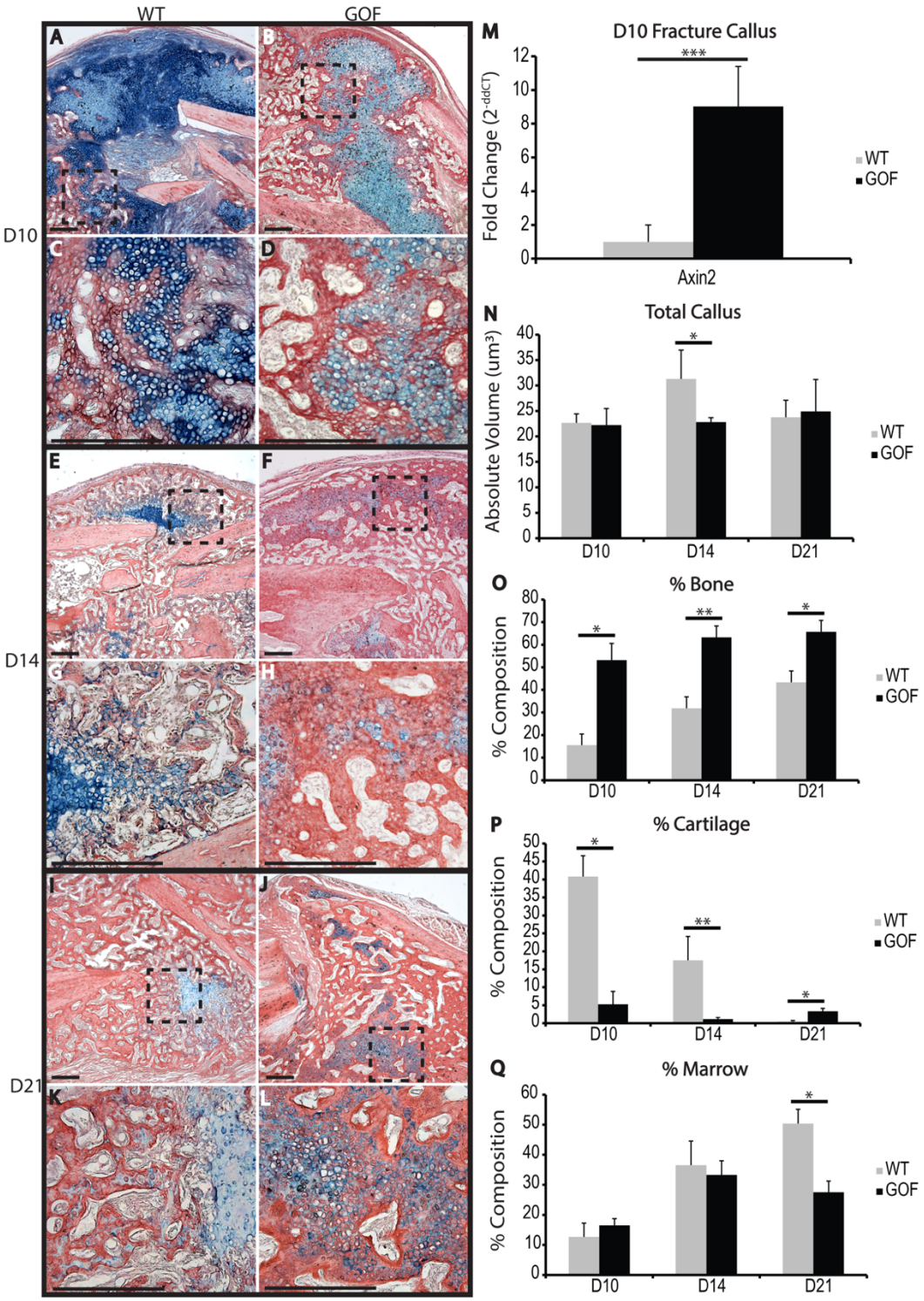

Figure 3.7: Overactivation of Canonical Wnt Signaling through Induced Stabilization of β-catenin in Chondrocytes Significantly Increases Bone Formation and Accelerates Endochondral Healing Stereological quantification (M-Q) of HBQ histology (A-L) reveals that over-activation of canonical Wnt signaling through the conditional stabilization of β-catenin in chondrocytes significantly increases and accelerates trabecular bone formation at early time points (D10, N). HBQ histology: cartilage = blue, bone = red. N=5/group/time point. Scale = 1000μm. (*) = p< 0.05. (**) = p< 0.01.

Callus Macrophages, Chondrocytes, and Endothelial Cells Express Wnt Ligands:

The chondro-osseous border of the fracture callus is hallmarked by the invasion of blood vessels **(**"Transition Zone", **Figure 3.8, A)**, and we have previously shown that paracrine signaling from endothelial cells can stimulate chondrocytes to mineralize their surrounding matrix.[1] In order to understand whether this may be due to endothelial cell secretion of Wnts, we treated 293-STF luciferase Wnt reporter cells with 20% human umbilical vein endothelial cell (HUVEC)-conditioned media. HUVEC-conditioned media produced the same level of Wnt pathway activation as treatment with 2nM Wnt3a and significantly higher activation compared to mock treatment **(Figure 3.8, B)**. Furthermore, RT-PCR analysis of HUVECs demonstrated that these cells express Wnts 3 and 7b as well as R-spondin 3, one of the four R-spondin secreted agonists responsible for the potentiation of Wnt signaling **(Figure 3.8, C)**.[122] Thus, endothelial cells are not only capable of releasing Wnts but are also able to activate canonical Wnt signaling.

To confirm that endothelial cells express Wnts in the biological context of fracture repair and to identify other potential sources of Wnts, gene expression analysis of Wnt ligands was performed on FACS-sorted callus macrophages, chondrocytes, and endothelial cells, as well as total callus CD45+ and CD45- cell populations. Endothelial cells (CD31+, Ve-Cadherin+), macrophages (CD45+, F4/80+, CD11b+), and total callus CD45+ and CD45- cell populations were isolated from C57BL/6 mice at 14 days post-fracture. Chondrocytes (tdTomato+, CD45-) were isolated from Aggrecan-Cre^{ERT2}::tdTomato HZE reporter mice at 10 days post-fracture in order to obtain as pure a population of chondrocytes as possible. The cartilage intermediate reaches its greatest size and the callus primarily consists of cartilage at 10 days post-fracture. All cell populations expressed numerous Wnt ligands, with endothelial cells followed by chondrocytes expressing the greatest number of Wnts and CD45+ cells expressing the fewest **(Figure 3.8, D-E).** Although endothelial cells expressed the greatest variety of Wnts, the total callus CD45- cell population expressed the

greatest quantity of Wnts as demonstrated by the comparison of gene expression levels for Wnt 10b, the most highly-expressed Wnt within the fracture callus **(Figure 3.8, E)**.

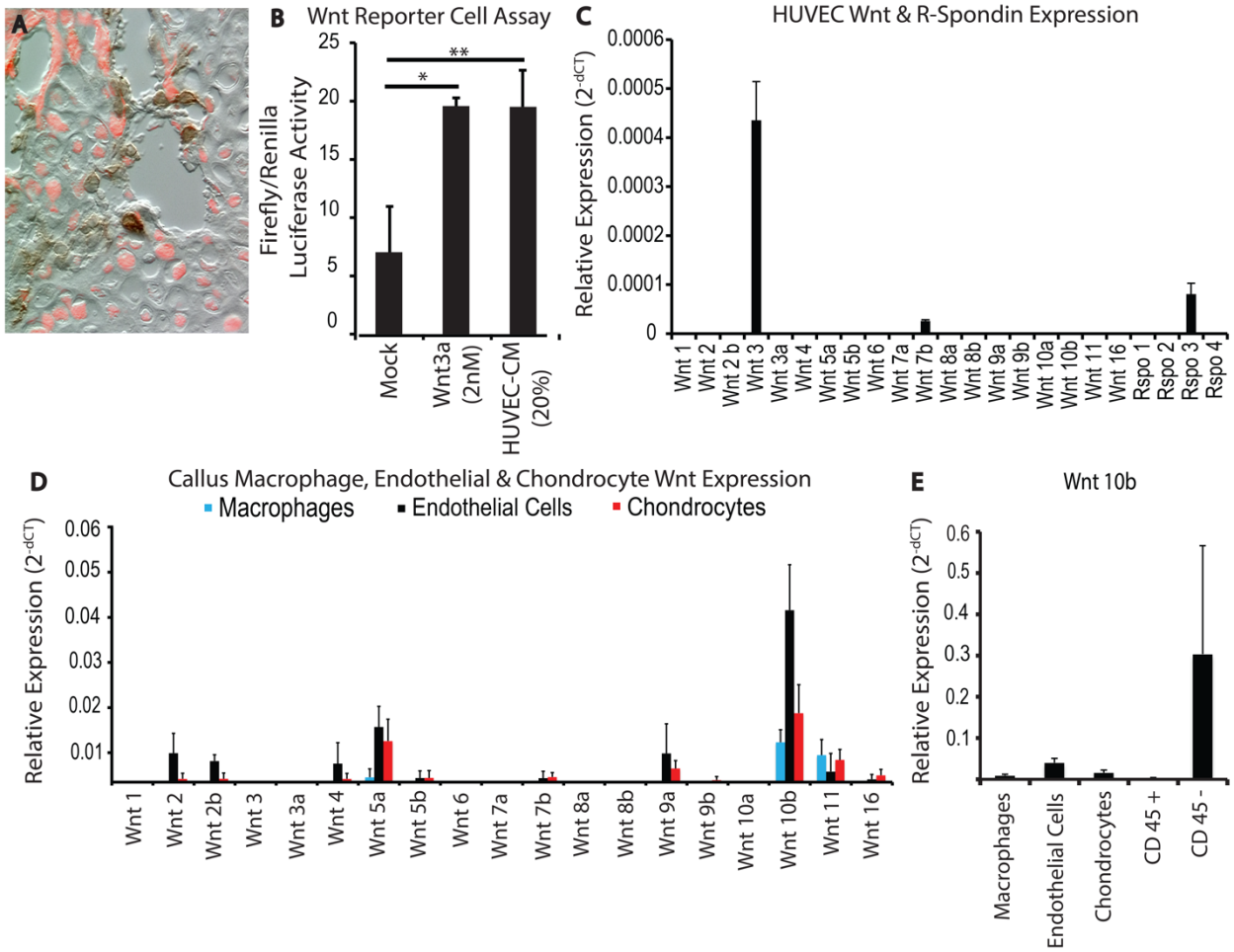

Figure 3.8: *In Vitro* and *In Vivo* Wnt Pathway Analysis. The Transition Zone is hallmarked not only by the chondro-osseous border where callus cartilage joins the newly-formed bone but also by the presence of macrophages and invading blood vessels (A, tdTomato+ = chondrocytes, brown = F4/80 IHC). Secreted factors from human umbilical vein endothelial cells (HUVECs) were capable of activating canonical Wnt signaling as evidenced by the significant increase in luciferase activity of 293-STF Wnt reporter cells treated with 20% HUVEC-conditioned media (HUVEC-CM) compared to mock control (B). The level of Wnt pathway activity induced with 20% HUVEC-CM was similar to that due to treatment with 2nM Wnt3a (B) (N=11 batches of HUVEC-CM, each tested twice in triplicate). HUVEC RT-PCR analysis revealed expression of Wnt 3, 7b, and R-spondin 3 (C) (N=3). In the context of fracture repair, callus macrophages, endothelial cells, and chondrocytes also expressed numerous Wnts (D) (N=3/cell population). Although endothelial cells, followed by chondrocytes, expressed the greatest variety of Wnts, the CD45- cell population expressed the greatest quantity of Wnt ligands, as evidenced by the relative expression of Wnt10b, the most highly expressed ligand (E) (N=3/cell population). (*) = $p < 0.05$. (**) = $p < 0.01$.

Canonical Wnt Pathway Activation in Callus Chondrocytes is independent of Porcupine:

In order to test the functional role of Wnt ligands in activating canonical Wnt signaling in callus chondrocytes we conditionally deleted the O-acyltransferase Porcupine, which is required for Wnt palmitoylation, intracellular transport and secretion.[56,111–113] Since endothelial cells and chondrocytes expressed significantly more Wnt ligands compared to macrophages, we limited our study to the deletion of Porcupine from endothelial cells using an inducible Ve-Cadherin Cre^{ERT2} (Cdh5(PAC)-CreERT2) mouse **(Figure 3.9)** and from chondrocytes using the inducible Aggrecan-Cre^{ERT2} mouse **(Figure 3.10).** The specificity of the Ve-Cadherin Cre^{ERT2} mouse in targeting endothelial cells was confirmed by performing lineage tracing analysis with a tdTomato reporter and through double-labelling of endothelial cells through PECAM immunohistochemistry **(Figure 3.11).** tdTomato fluorescence was robust throughout the marrow region. Within the fracture callus, tdTomato fluorescence it was only observed at the Transition Zone border of the cartilage callus, as would be expected since cartilage is an avascular tissue. PECAM immunohistochemical staining closely followed tdTomato expression **(Figure 3.11).**

Deletion of Porcupine from endothelial cells did not result in a significant change in absolute volume for bone or cartilage **(Figure 3.9)**. However, it did result in a slight increase in callus size, which is likely the cause of the small, but statistically significant, decrease in % bone composition **(Figure 3.9)**. This reported difference in bone formation is minimal compared to the drastic reduction in bone formation upon deletion of β-catenin from chondrocytes. Indeed, the histology images in **Figure 3.9, E-H** depict regions within the fracture callus that have the greatest histological variation in bone formation between treatment groups following deletion of Porcupine from endothelial cells. This difference in bone formation is negligible compared to the reduction in bone due to loss of β-catenin in chondrocytes. Deletion of Porcupine in chondrocytes did not result in any statistically significant changes **(Figure 3.10)**.

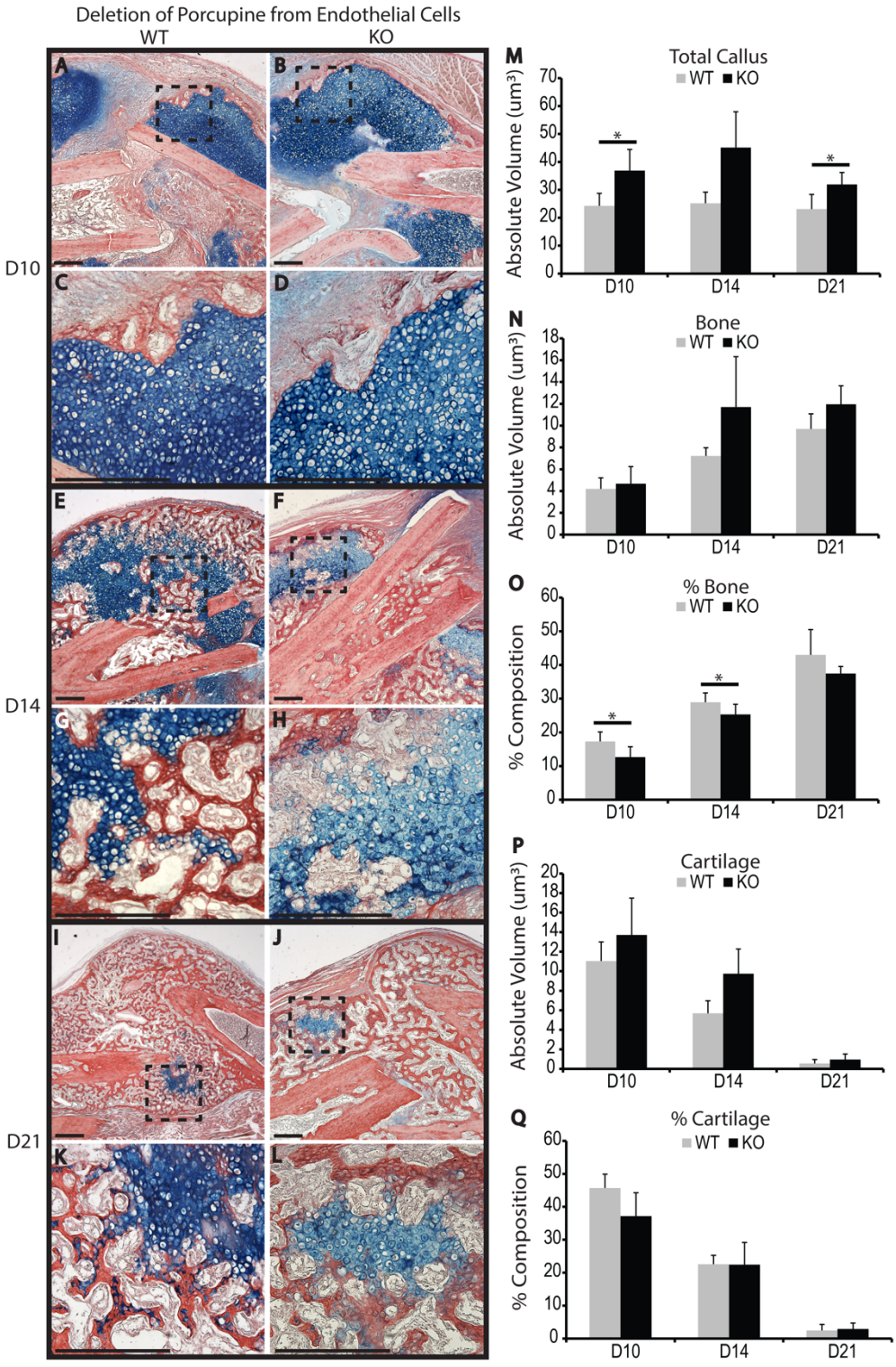

Figure 3.9: Inhibition of Porcupine in Endothelial Cells does not Significantly alter Absolute Volume of Bone or Cartilage. Stereological quantification (M-Q) of HBQ histology (A-L) reveals that inhibition of Porcupine in endothelial cells using an inducible Ve-Cadherin Cre does not significantly alter the absolute volume of callus bone or cartilage (N, P). However, it did result in a slight increase in callus size (M), which is likely the cause of the small but statistically significant

decrease in % bone composition (O). The difference in bone formation due to deletion of Porcupine in endothelial cells is minimal compared to the stark reduction in bone formation upon deletion of β-catenin from chondrocytes. Indeed, the histology images in E-H depict regions within the fracture callus that have the greatest histological variation in bone formation between treatment groups following deletion of Porcupine from endothelial cells. HBQ histology: cartilage = blue, bone = red. N=5/group/time point. Scale = 1000μm. (*) = p< 0.05.

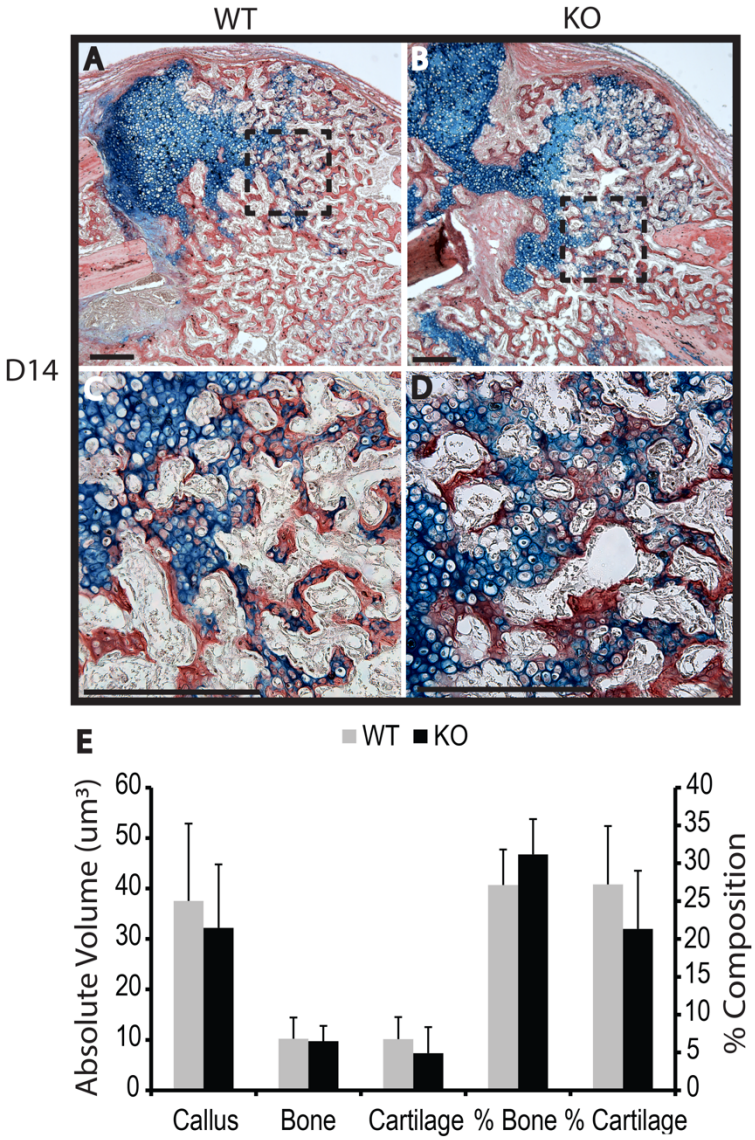

Figure 3.10: Deletion of Porcupine in Callus Chondrocytes does Not Significantly Alter Any Callus Tissue Composition Parameters. Stereological quantification (E) of HBQ histology (A-D) reveals that deletion of Porcupine from chondrocytes does not significantly alter any tissue parameters (E). N=5/group.

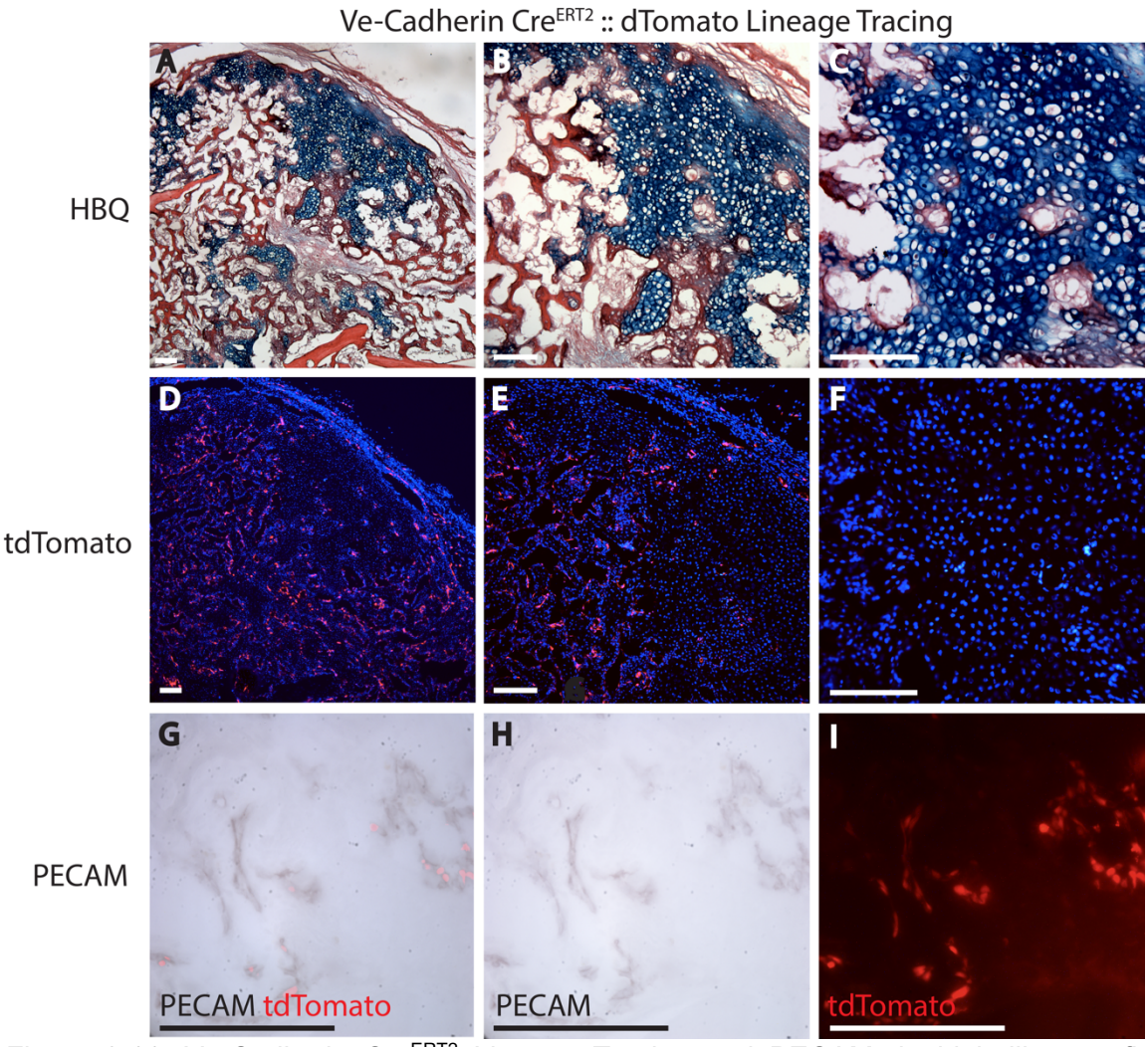

Figure 3.11: Ve-Cadherin Cre^{ERT2} Lineage Tracing and PECAM dual-labelling confirms Cre specificity. Lineage tracing of Ve-Cadherin Cre^{ERT2} mice using a tdTomato reporter demonstrated endothelial-specific labelling. tdTomato fluorescence was robust within the marrow cavity (A-B, D-E). However, it was only observed in cartilage at the Transition Zone regions where the callus cartilage joins the newly-formed bone (C,F). This is as expected since cartilage is an avascular tissue that recruits the vasculature at the Transition Zone during chondrocyte-to-osteoblast transformation. PECAM immunohistochemistry closely paralleles tdTomato fluorescence (G-I, G = combined, H = PECAM IHC only, I = tdTomato only). N=3. Scale = 400μm.

Given that numerous cell sources of Wnts might produce a compensatory effect, we sought to determine the effect of reducing Wnt ligand palmitoylation globally by conditionally deleting Porcupine using the R26-Cre^{ERT2} mouse. Cre recombination was induced as previously with daily injections of Tamoxifen from days six to ten post-fracture. Global deletion of Porcupine did not result in any statistically significant difference in callus size or tissue composition **(Figure 3.12)**.

Porcupine deletion was confirmed using callus tissues harvested by microdissection from adjacent paraffin sections of the same specimens used for stereological analysis. RT-PCR analysis was performed using primers (P1-P4) designed to recognize the floxed-deleted Porcupine allele sequence **(Figure 3.12, F, H)**.[119] Significant amplification of the floxed-deleted sequence was observed for experimental samples, indicating that Cre recombination took place **(Figure 3.12, F, H)**. In contrast, no amplification of the floxed-deleted sequence was observed in control samples possessing the wildtype Porcupine allele **(Figure 3.12, F, H)**.

To determine Cre recombination efficiency, RT-PCR analysis was performed using primer pairs (P1-P2 and P3-P4) designed to amplify non-recombined Porcupine alleles (both wildtype and non-recombined floxed).[119] Since Porcupine is X-linked and only male mice were used in this experiment, Cre recombination was maximized and the degree of sequence amplification reflects the relative proportion of cells that failed to undergo recombination. Cre recombination efficiency was calculated by comparing sequence amplification in control samples possessing the wildtype Porcupine allele (100% no recombination) with that of experimental samples possessing the floxed allele. Control samples had 2.83 fold greater amplification of the P1-P2 sequence and 4.44 fold greater amplification of the P3-P4 sequence compared to experimental samples, indicating that experimental samples underwent significant recombination compared to controls (65-77%) **(Figure 3.12, G).** Together, this data confirm that Porcupine was deleted globally with high efficiency and that Porcupine-mediated post-translational modification of Wnts is not required for β-catenin activation in chondrocytes and chondrocyte-to-osteoblast transformation.

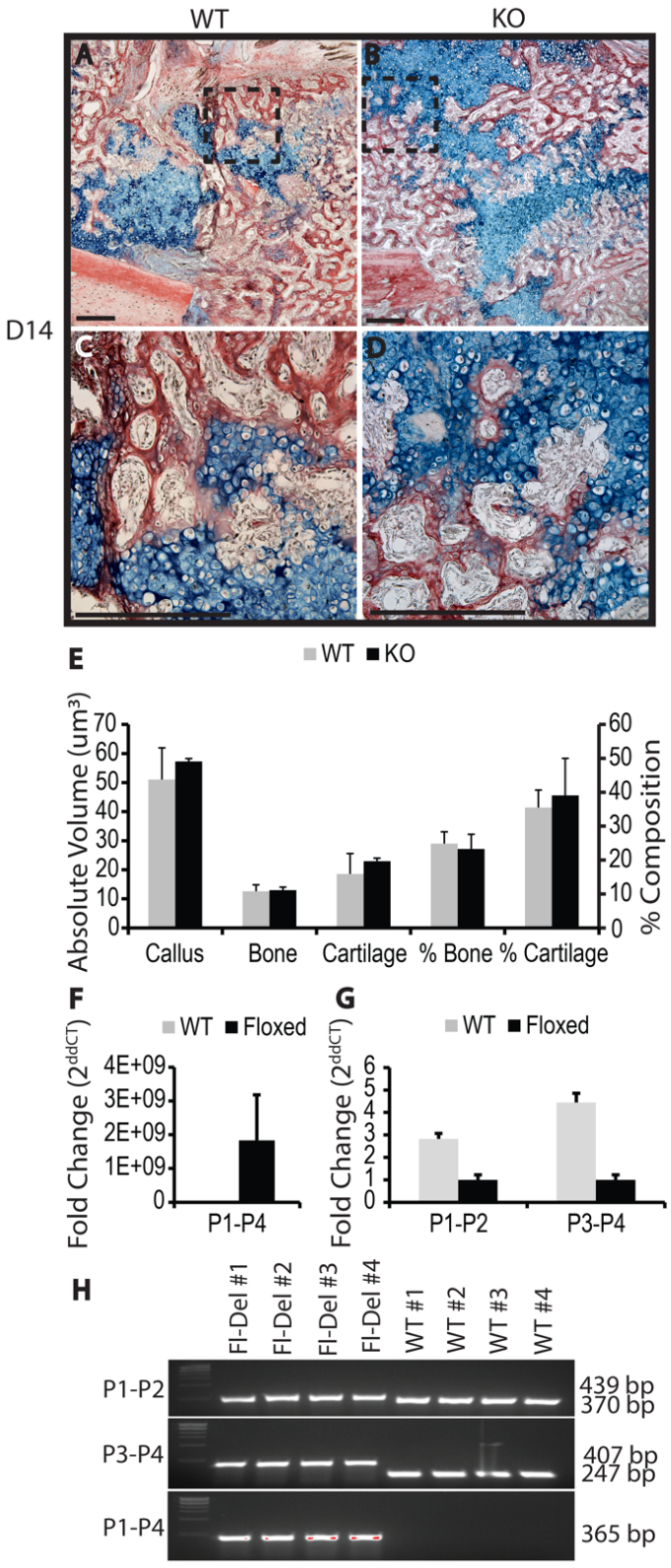

Figure 3.12: Global Inhibition of Porcupine does not Significantly alter Callus Tissue Composition. Stereological quantification (E) of HBQ histology (A-D) demonstrates that global deletion of Porcupine does not significantly alter callus size or tissue composition (E). RT-PCR analysis using

primers (P1-P4) designed by Liu *et al.* to recognize the floxed-deleted Porcupine allele sequence confirms Porcupine deletion in experimental samples (F, H). The specificity of this primer pair is evidenced by the lack of sequence amplification in control samples, which do not possess the floxed allele. Cre recombination efficiency was calculated based on RT-PCR analysis using primer pairs (P1-P2 and P3-P4) designed to recognized non-recombined alleles (both wildtype and non-recombined floxed) (G, H). Control samples possessing the wildtype Porcupine allele (100% no recombination) had 2.83 fold greater amplification of the P1-P2 sequence and 4.44 fold greater amplification of the P3-P4 sequence compared to experimental samples, resulting in a Cre recombination efficiency of 65-77% (G). Together, this data confirms that Porcupine was deleted globally with high efficiency and that Porcupine-mediated post-translational modification of Wnts is not required for β-catenin activation in chondrocytes and, consequently, chondrocyte-to-osteoblast transformation. N=5/group.

DISCUSSION:

Numerous genetic lineage tracing studies have demonstrated that chondrocytes directly contribute to endochondral bone formation by transforming into osteoblasts.[17,22–24,79,86,87] This has been shown in the contexts of bone development, postnatal growth, and fracture repair with an array of reporter systems (Col10-Cre, Col2-Cre^{ERT2}, Aggrecan-Cre^{ERT2}, eGFP- and β-galactosidase-labelled tissue transplants).[17,22–24,79,86,87] However, the signaling mechanisms that regulate the process of chondrocyte-to-osteoblast transformation remain largely unknown.

Canonical Wnt signaling has been repeatedly shown to promote osteogenesis in the context of intramembranous bone repair.[47–49] Pathway inhibition through adenoviral expression of Dkk1 significantly reduces bone formation in transcortical defect models, which heal through intramembranous ossification.[47] Conversely, activation of canonical Wnt signaling through deletion of pathway inhibitors (Sclerostin, Axin2) significantly increases intramembranous bone formation.[48] However, canonical Wnt signaling in endochondral repair has been less explored.

Interestingly, during development, the canonical Wnt pathway has been shown to act as a "molecular switch" by promoting osteogenic differentiation while repressing chondrogenic cell fate decisions.[44–46] Inhibition of canonical Wnt signaling through deletion of β-catenin from skeletogenic mesenchyme results in early osteoblast differentiation arrest and ectopic cartilage

formation.[44,46] Similar results have been reported from *in vitro* experiments that inhibit canonical Wnt signaling in mesenchymal progenitor cells.[44] Recently, Houben *et al.* demonstrated that canonical Wnt signaling also serves as a molecular regulator of chondrocyte-to-osteoblast transformation during endochondral bone development.[24] Deletion of β-catenin from hypertrophic chondrocytes using a *Col10a1*-Cre resulted in significantly reduced bone formation, whereas induced expression of an indestructible form of β-catenin produced osteopetrotic bone.[24]

Numerous Wnt ligands, receptors, and components of the transduction machinery have been shown to be expressed during endochondral healing, but their functional role remains unclear.[43,50] Our data indicate that β-catenin and canonical Wnt signaling in fracture callus chondrocytes is critical to chondrocyte-to-osteoblast transformation during endochondral repair. Conditional deletion of β-catenin using an inducible Aggrecan-Cre resulted in significantly reduced new bone formation and increased cartilage retention. This confirms work from a similar study using Col2a1-ICAT transgenic mice to inhibit canonical Wnt signaling in chondrocytes that found delayed cartilage and reduced bone formation following tibia fracture.[51] Importantly, our data indicate that inhibition of canonical Wnt signaling does not increase chondrocyte cell death. This confirms previously published evidence demonstrating that cell death is not the exclusive fate of hypertrophic chondrocytes.[17,24] Indeed, our tdTomato lineage tracing analysis following deletion of β-catenin in callus chondrocytes revealed that tdTomato positive cells detach from their cartilage matrix and remain within the marrow cavity up to 35 days post-fracture.

It is possible that the prolonged presence of tdTomato+ cells within the marrow cavity is due to the phagocytic activity of hematopoietic cells that have engulfed dying chondrocytes. FACS analysis of tdTomato positive cells isolated from the marrow cavity following deletion of β-catenin revealed a subset of cells that were also positive for CD45, a marker of hematopoietic cell lineages.[120,121] Significant dual tdTomato+ and CD45+ labelling was only observed upon deletion

of β-catenin. Control marrow cells possessing the tdTomato reporter and wildtype copies of β-catenin had little to no dual-labelled cells. Furthermore, the number of dual-labelled cells found in control samples was similar to that found in wildtype mice that did not possess the tdTomato reporter. Thus, tdTomato and CD45 analysis were highly specific. Hematopoietic engulfment of detached chondrocytes is reminiscent of efferocytosis, a mechanism used by phagocytic cells to remove cellular debris for the resolution of tissue damage and during normal tissue development.[123,124] Phagocytosis is mediated by professional and non-professional phagocytic cells including macrophages, dendritic cells, tissue-infiltrating monocytes, neutrophils, and eosinophils as well as epithelial cells of mammary epithelium and astrocytes in the brain.[124–126] However, in the majority of cases, phagocytic clearance is primarily done by macrophages.[123] This is likely the case in the context of hematopoietic engulfment of chondrocytes during fracture repair, since we show macrophages are present at the Transition Zone.

The canonical Wnt pathway is an important regulator of osteoclastogenesis.[127] Inhibition of β-catenin in hypertrophic chondrocytes during bone development impairs trabecular bone formation and is associated with enhanced subchondral osteoclast number and increased expression of *receptor activator of nuclear factor kappa-B ligand* (*Rankl*), which is known to stimulate osteoclastogenesis.[127] Houben *et al.* demonstrated that modulation of canonical Wnt signaling in chondrocytes affects osteoclastogenesis by altering the expression of *Rankl* and *Osteoprotegrin* (*Opg*), a Rankl antagonist.[24] They also demonstrated that downregulation or increased activation of osteoclastogenesis was able to partially rescue the phenotypic changes observed from loss or stabilization of β-catenin, respectively.[24] Our data indicate that β-catenin and the canonical Wnt pathway may play a similar role during endochondral repair. TRAP staining revealed that deletion of β-catenin increased the localization of TRAP-positive cells to the border of the cartilage callus. This localized increase in osteoclastic activity may be responsible for the robust detachment of tdTomato+ cells observed within the marrow cavity.

In contrast to deletion of β-catenin signaling in callus chondrocytes, pathway gain-of-function through conditional expression of an indestructible form of β-catenin resulted in increased and accelerated bone formation. This increase in bone formation corresponded with a simultaneous decrease in callus cartilage composition, indicating that canonical Wnt signaling is responsible for regulating chondrocyte-to-osteoblast transformation. Chondrocyte transformation is known to occur in a specific region of the fracture callus, which we have termed the "Transition Zone" as this is where the callus cartilage joins the newly formed bone.[17,23] Previously we showed that hypertrophic chondrocytes at the Transition Zone express transcription factors traditionally associated with stem cell pluripotency (Sox2, Oct4, Nanog).[17] Importantly, we demonstrated that *Sox2* plays a functional role in fracture repair with deletion of *Sox2* during the cartilaginous phase of healing resulting in significantly reduced new bone formation and increased cartilage retention within the fracture callus.[17] It is unlikely that chondrocytes truly become pluripotent during transformation, but we suggest that *Sox2* may play a role in chondrocyte plasticity. Recently, Willet *et al.* coined the term "paligenosis" to describe the process by which differentiated cells revert to a proliferative and regenerative state and undergo metaplasia in response to tissue injury in the context of stomach and pancreatic regeneration.[128] Our data suggest a similar process occurs in the context of fracture repair.

Our data support the concept that vascular invasion is a critical regulator of paligenosis during endochondral fracture repair. Secreted factors from human umbilical vein endothelial cells (HUVECs) induce expression of pluripotency transcription factors (*sox2, oct4, nanog*) and the osteogenic gene o*steocalcin* in fracture callus explants.[17] Here we demonstrated that HUVEC-secreted factors are also capable of stimulating canonical Wnt signaling using the luciferase-based 293-STF Wnt reporter cells, and qPCR analysis of HUVECs reveals that these cells express numerous Wnts and R-Spondins. Cells isolated from fracture calli by FACS also revealed significant expression of a variety of Wnt ligands. Endothelial cells, macrophages, and

chondrocytes were isolated along with total callus CD45+ and CD45- cell populations. All populations expressed numerous Wnt ligands, with CD45- cells expressing a significantly larger quantity and variety of Wnts compared to CD45+ cells and with endothelial cells followed by chondrocytes expressing the most Wnts out of the three specifically-isolated cell types. Taken together these data suggest that multiple cell types may contribute to the production of Wnt ligands for promoting the osteogenic switch within chondrocytes.

To determine which source of Wnt ligands was most critical to fracture repair we conditionally deleted Porcupine from chondrocytes, endothelial cells, or globally.[56,111–113] Porcupine is an O-acyltransferase required for Wnt palmitoylation, intracellular transport, and secretion.[56,111–113] Interestingly, deletion of Porcupine produced no significant effect on fracture callus composition in any of these conditions. Global porcupine deletion was confirmed with Cre recombination efficiency estimated at 65-77% using primers designed by Liu *et al.* to recognize non-recombined allele sequences (both wildtype and non-recombined floxed alleles).[119] Given that a statistically significant change in cartilage-to-bone conversion was observed when only one copy of β-catenin was deleted from chondrocytes, the high rate of Porcupine Cre recombination suggests that post-translational modification of Wnts via Porcupine is not required for β-catenin activation during chondrocyte-to-osteoblast transformation.

It is possible that β-catenin activation during chondrocyte-to-osteoblast transformation is Wnt ligand-independent. Numerous studies conducted in a variety of biological contexts have demonstrated that the canonical Wnt pathway can be activated in a ligand-independent manner.[89] The majority of Wnt ligand-independent pathways increase the signaling capacity of β-catenin through dissociation of β-catenin from its membrane-associated complex with α-catenin and cadherins through a variety of receptor tyrosine kinases (RTKs), including EGFR,[89–92] FGFR2,[93–95] FGFR3,[93] FGFR4,[96] TRKA,[93] IGFR1,[97–99] and VEGFR2.[100,101] Non-RTK mechanisms have also

been shown to regulate β-catenin activity including c-Src[92,102,103], PTEN,[104,105] caveolin-1 (CAV1),[104,106,107] and plakoglobin (γ-catenin).[108–110] In the context of fracture repair, although it is possible that deletion of β-catenin in chondrocytes alters cell-cell adhesion mediated by β-catenin complexes and causes decreased bone formation, this is unlikely since gain-of-function experiments show accelerated healing and Axin2, a transcriptional readout of Wnt signaling, is up-regulated by callus chondrocytes. Together, these observations suggest that the effect of β-catenin in chondrocytes during fracture healing is via its transcriptional activation of target genes. Identifying these targets is the focus or our current work.

Further analysis is required to confirm that β-catenin activation in chondrocytes during transformation and endochondral repair is truly Wnt ligand-independent. Numerous studies have indicated that Porcupine and Wntless are essential mediators of Wnt secretion and signaling.[129] However, additional studies report phenotypic differences in loss-of-function experiments comparing these two genes.[129] Thus, although our data clearly demonstrate that porcupine-mediated modification of Wnt ligands is not required for β-catenin activation in chondrocytes, it is possible that Wnt ligands may still play an important role in activating β-catenin.

Together, our data demonstrate the critical role of β-catenin/Wnt signaling to the process of chondrocyte-to-osteoblast transformation and the independence of β-catenin activity from Porcupine-mediated post-translational modification. These data provide important insight towards a complete understanding of the process of endochondral repair. **Figure 3.13** outlines our current understanding of this process to date. Future work is necessary to determine the molecular signals that activate chondrocyte β-catenin activity.

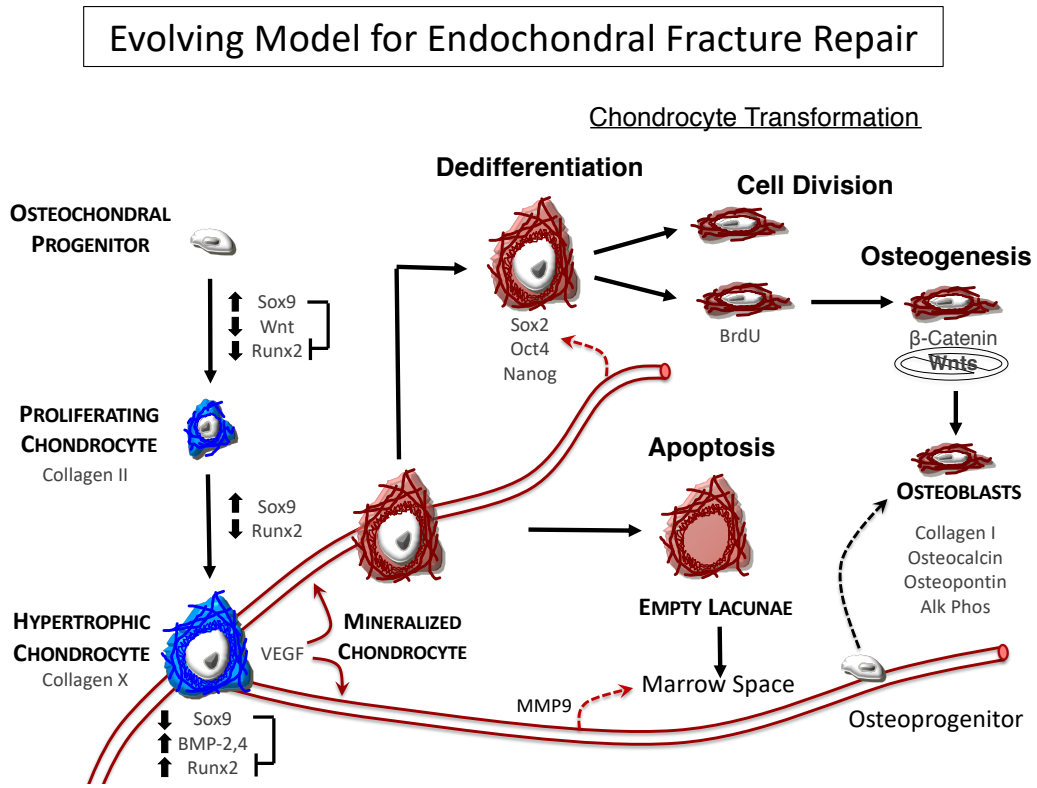

Figure 3.13: New Model for Endochondral Fracture Repair. Evidence from this study contributes to our greater understanding of endochondral repair. This process begins with the differentiation of osteochondral progenitor cells, which differentiate into chondrocytes that proliferate to form the cartilage callus. Chondrocytes then undergo hypertrophy, recruit the vasculature and mineralize their surrounding matrix. A portion of chondrocytes undergo apoptosis in order to make room for the marrow cavity. However, a significant population of chondrocytes survive and transform into osteoblasts that will contribute to the formation of new bone. During the process of chondrocyte transformation, cells express pluripotency transcription factors, undergo cell division, and activate the canonical Wnt pathway independent of Porcupine-mediated Wnt palmitoylation.

CONCLUSION:

Our data demonstrate the key role of β-catenin and the canonical Wnt pathway in chondrocyte-to-osteoblast transformation during endochondral repair. We show that canonical Wnt signaling is not required for chondrocyte survival but rather that this pathway likely functions to regulate gene expression for cell programing and osteoclastogenesis. Furthermore, we demonstrate that although numerous Wnt ligands are expressed by multiple tissues within the fracture callus, their role in mediating Wnt pathway activation in chondrocytes may be limited and is independent of Porcupine-mediated post-translational modification.

SUPPLEMENTARY INFORMATION:

Table 3.1: SYBR Green Primers for Gene Expression Analysis

Primer	Species	Company	Sequence
Axin2 Forward	Mouse	Thermo	5'- CTCCCCACCTTGAATGAAGA -3'
Axin2 Reverse	Mouse	Thermo	5'- ACTGGGTCGCTTCTCTTGAA -3'

Table 3.2: TaqMan Assays Used for Gene Expression Analysis

Gene	Species	Company	Catalog #	Assay ID
18S	Human	Thermo	4331182	Hs99999901_s1
beta-actin (ACTB)	Mouse	Thermo	4453320	Mm01205647_g1
GAPDH	Human	Thermo	4453320	Hs02758991_g1
GAPDH	Mouse	Thermo	4331182	Mm99999915_g1
Rspo1	Mouse/Human	Thermo	4453320	Mm00507077_m1
Rspo2	Mouse	Thermo	4453320	Mm00555790_m1
Rspo2	Human	Thermo	4448892	Hs04400416_m1
Rspo3	Mouse/Human	Thermo	4453320	Mm01188251_m1
Rspo4	Mouse/Human	Thermo	4453320	Mm00615419_m1
Wnt1	Mouse/Human	Thermo	4453320	Mm01300555_g1

Gene	Species	Company	Catalog #	Assay ID
Wnt10a	Mouse/Human	Thermo	4331182	Mm00437325_m1
Wnt10b	Mouse/Human	Thermo	4453320	Mm00442104_m1
Wnt11	Mouse/Human	Thermo	4453320	Mm00437328_m1
Wnt16	Mouse	Thermo	4453320	Mm00446420_m1
Wnt16	Human	Thermo	4453320	Hs00365138_m1
Wnt2	Mouse/Human	Thermo	4453320	Mm00470018_m1
Wnt2b (Wnt13)	Mouse/Human	Thermo	4453320	Mm00437330_m1
Wnt3	Mouse	Thermo	4453320	Mm00437336_m1
Wnt3	Human	Thermo	4448892	Hs00902257_m1
Wnt3a	Mouse	Thermo	4453320	Mm00437337_m1
Wnt3a	Human	Thermo	4453320	Hs00263977_m1
Wnt4	Mouse/Human	Thermo	4453320	Mm01194003_m1
Wnt5a	Mouse/Human	Thermo	4453320	Mm00437347_m1
Wnt5b	Mouse/Human	Thermo	4453320	Mm01183986_m1
Wnt6	Mouse/Human	Thermo	4448892	Mm00437351_m1
Wnt7a	Mouse/Human	Thermo	4453320	Mm00437356_m1

Gene	Species	Company	Catalog #	Assay ID
Wnt7b	Mouse	Thermo	4453320	Mm01301717_m1
Wnt7b	Human	Thermo	4453320	Hs00536497_m1
Wnt8a	Mouse/Human	Thermo	4453320	Mm01157914_g1
Wnt8b	Mouse/Human	Thermo	4453320	Mm00442108_g1
Wnt9a	Mouse/Human	Thermo	4453320	Mm00460518_m1
Wnt9b	Mouse/Human	Thermo	4453320	Mm00457102_m1

Table 3.3: Antibodies Used for FACS

Target	Fluorofore	Company & Catalog #
CD11b	PeCy7	BD #552850
CD31	FITC	Biolegend #102406
CD45	FITC	BD #553080
F4/80	APC	eBioscience #17480182
Ve-Cadherin (CD144)	PeCy7	Biolegend #138016
VEGFR2 (CD309)	APC	Biolegend #136405

References

1. Bahney, C. S., Hu, D. P., Miclau, T. & Marcucio, R. S. The multifaceted role of the vasculature in endochondral fracture repair. *Bone Res.* **6**, 4 (2015).
2. Thompson, Z., Miclau, T., Hu, D. & Helms, J. A. A model for intramembranous ossification during fracture healing. *J. Orthop. Res.* **20**, 1091–1098 (2002).
3. Colnot, C. Skeletal Cell Fate Decisions Within Periosteum and Bone Marrow During Bone Regeneration. *J. Bone Miner. Res.* **24**, 274–282 (2009).
4. Duchamp de Lageneste, O. *et al.* Periosteum contains skeletal stem cells with high bone regenerative potential controlled by Periostin. *Nat. Commun.* **9**, 773 (2018).
5. Silkstone, D., Hong, H. & Alman, B. A. Beta-catenin in the race to fracture repair: in it to Wnt. *Nat. Clin. Pract. Rheumatol.* **4**, 413–419 (2008).
6. Xing, Z., Lu, C., Hu, D., Miclau, T. & Marcucio, R. S. Rejuvenation of the inflammatory system stimulates fracture repair in aged mice. *J. Orthop. Res.* **28**, 1000–1006 (2010).
7. Wray, J. B. Acute Changes in Femoral Arterial Blood Flow after Closed Tibial Fracture in Dogs. *JBJS* **46**, 1262 (1964).
8. Park, S.-H., Silva, M., Bahk, W.-J., McKellop, H. & Lieberman, J. R. Effect of repeated irrigation and debridement on fracture healing in an animal model. *J. Orthop. Res.* **20**, 1197–1204 (2002).
9. Kronenberg, H. M. Developmental regulation of the growth plate. *Nature* **423**, 332–336 (2003).
10. Long, F. & Ornitz, D. M. Development of the Endochondral Skeleton. *Cold Spring Harb. Perspect. Biol.* **5**, (2013).
11. Akiyama, H., Chaboissier, M.-C., Martin, J. F., Schedl, A. & de Crombrugghe, B. The transcription factor Sox9 has essential roles in successive steps of the chondrocyte differentiation pathway and is required for expression of Sox5 and Sox6. *Genes Dev.* **16**, 2813–2828 (2002).

12. Bi, W., Deng, J. M., Zhang, Z., Behringer, R. R. & Crombrugghe, B. de. *Sox9* is required for cartilage formation. *Nat. Genet.* **22**, 85 (1999).
13. Bell, D. M. *et al.* SOX9 directly regulates the type-ll collagen gene. *Nat. Genet.* **16**, 174 (1997).
14. Sekiya, I. *et al.* SOX9 enhances aggrecan gene promoter/enhancer activity and is up-regulated by retinoic acid in a cartilage-derived cell line, TC6. *J. Biol. Chem.* **275**, 10738–10744 (2000).
15. Gerber, H.-P. *et al.* VEGF couples hypertrophic cartilage remodeling, ossification and angiogenesis during endochondral bone formation. *Nat. Med.* **5**, 623 (1999).
16. Grässel, S. The role of peripheral nerve fibers and their neurotransmitters in cartilage and bone physiology and pathophysiology. *Arthritis Res. Ther.* **16**, (2014).
17. Hu, D. P. *et al.* Cartilage to bone transformation during fracture healing is coordinated by the invading vasculature and induction of the core pluripotency genes. *Development* **144**, 221–234 (2017).
18. Tatsuyama, K., Maezawa, Y., Baba, H., Imamura, Y. & Fukuda, M. Expression of various growth factors for cell proliferation and cytodifferentiation during fracture repair of bone. *Eur. J. Histochem. EJH* **44**, 269–278 (2000).
19. Cooper, K. L. *et al.* Multiple phases of chondrocyte enlargement underlie differences in skeletal proportions. *Nature* **495**, 375 (2013).
20. Hall, B. K. *Bones and Cartilage: Developmental and Evolutionary Skeletal Biology*. (Academic Press, 2014).
21. Chondroid Bone, Secondary Cartilage and Metaplasia. William A. Beresford , Maurizio Pacifici. *Q. Rev. Biol.* **56**, 471–471 (1981).
22. Yang, L., Tsang, K. Y., Tang, H. C., Chan, D. & Cheah, K. S. E. Hypertrophic chondrocytes can become osteoblasts and osteocytes in endochondral bone formation. *Proc. Natl. Acad. Sci. U. S. A.* **111**, 12097–12102 (2014).

23. Bahney, C. S. *et al.* Stem cell-derived endochondral cartilage stimulates bone healing by tissue transformation. *J. Bone Miner. Res. Off. J. Am. Soc. Bone Miner. Res.* **29**, 1269–1282 (2014).
24. Houben, A. *et al.* β-catenin activity in late hypertrophic chondrocytes locally orchestrates osteoblastogenesis and osteoclastogenesis. *Development* **143**, 3826–3838 (2016).
25. Jing, Y. *et al.* Chondrocytes Directly Transform into Bone Cells in Mandibular Condyle Growth. *J. Dent. Res.* 0022034515598135 (2015) doi:10.1177/0022034515598135.
26. Park, J. *et al.* Dual pathways to endochondral osteoblasts: a novel chondrocyte-derived osteoprogenitor cell identified in hypertrophic cartilage. *Biol. Open* **4**, 608–621 (2015).
27. Zhou, X. *et al.* Chondrocytes Transdifferentiate into Osteoblasts in Endochondral Bone during Development, Postnatal Growth and Fracture Healing in Mice. *PLoS Genet.* **10**, (2014).
28. Hubble, M. J. W. Bone grafts. *Surg. Technol. Int.* **10**, 261–265 (2002).
29. Brigman, B. E., Hornicek, F. J., Gebhardt, M. C. & Mankin, H. J. Allografts about the Knee in Young Patients with High-Grade Sarcoma. *Clin. Orthop.* 232–239 (2004).
30. Katagiri, T. & Watabe, T. Bone Morphogenetic Proteins. *Cold Spring Harb. Perspect. Biol.* **8**, (2016).
31. Salazar, V. S., Gamer, L. W. & Rosen, V. BMP signalling in skeletal development, disease and repair. *Nat. Rev. Endocrinol.* **12**, 203–221 (2016).
32. Einhorn, T. A. The Wnt Signaling Pathway as a Potential Target for Therapies to Enhance Bone Repair. *Sci. Transl. Med.* **2**, 42ps36-42ps36 (2010).
33. Hoffmann, A. & Gross, G. BMP signaling pathways in cartilage and bone formation. *Crit. Rev. Eukaryot. Gene Expr.* **11**, 23–45 (2001).
34. Karsenty, G. & Wagner, E. F. Reaching a genetic and molecular understanding of skeletal development. *Dev. Cell* **2**, 389–406 (2002).

35. Chrastil, J., Low, J. B., Whang, P. G. & Patel, A. A. Complications Associated With the Use of the Recombinant Human Bone Morphogenetic Proteins for Posterior Interbody Fusions of the Lumbar Spine. *Spine* **38**, (2013).

36. Almubarak, S. *et al.* Tissue engineering strategies for promoting vascularized bone regeneration. *Bone* **83**, 197–209 (2016).

37. DeVine, J. G., Dettori, J. R., France, J. C., Brodt, E. & McGuire, R. A. The use of rhBMP in spine surgery: is there a cancer risk? *Evid.-Based Spine-Care J.* **3**, 35–41 (2012).

38. Dang, P. N. *et al.* Controlled Dual Growth Factor Delivery From Microparticles Incorporated Within Human Bone Marrow-Derived Mesenchymal Stem Cell Aggregates for Enhanced Bone Tissue Engineering via Endochondral Ossification. *Stem Cells Transl. Med.* **5**, 206–217 (2016).

39. Simmons, C. A., Alsberg, E., Hsiong, S., Kim, W. J. & Mooney, D. J. Dual growth factor delivery and controlled scaffold degradation enhance in vivo bone formation by transplanted bone marrow stromal cells. *Bone* **35**, 562–569 (2004).

40. Sukul, M., Nguyen, T. B. L., Min, Y.-K., Lee, S.-Y. & Lee, B.-T. Effect of Local Sustainable Release of BMP2-VEGF from Nano-Cellulose Loaded in Sponge Biphasic Calcium Phosphate on Bone Regeneration. *Tissue Eng. Part A* **21**, 1822–1836 (2015).

41. Krishnan, L. *et al.* Delivery vehicle effects on bone regeneration and heterotopic ossification induced by high dose BMP-2. *Acta Biomater.* **49**, 101–112 (2017).

42. Gammons, M. & Bienz, M. Multiprotein complexes governing Wnt signal transduction. *Curr. Opin. Cell Biol.* **51**, 42–49 (2018).

43. Chen, Y. *et al.* Beta-Catenin Signaling Plays a Disparate Role in Different Phases of Fracture Repair: Implications for Therapy to Improve Bone Healing. *PLoS Med* **4**, e249 (2007).

44. Hill, T. P., Später, D., Taketo, M. M., Birchmeier, W. & Hartmann, C. Canonical Wnt/β-Catenin Signaling Prevents Osteoblasts from Differentiating into Chondrocytes. *Dev. Cell* **8**, 727–738 (2005).

45. Topol, L., Chen, W., Song, H., Day, T. F. & Yang, Y. Sox9 inhibits Wnt signaling by promoting beta-catenin phosphorylation in the nucleus. *J. Biol. Chem.* **284**, 3323–3333 (2009).

46. Day, T. F., Guo, X., Garrett-Beal, L. & Yang, Y. Wnt/β-Catenin Signaling in Mesenchymal Progenitors Controls Osteoblast and Chondrocyte Differentiation during Vertebrate Skeletogenesis. *Dev. Cell* **8**, 739–750 (2005).

47. Kim, J.-B. *et al.* Bone Regeneration Is Regulated by Wnt Signaling. *J. Bone Miner. Res.* **22**, 1913–1923 (2007).

48. McGee-Lawrence, M. E. *et al.* Sclerostin deficient mice rapidly heal bone defects by activating β-catenin and increasing intramembranous ossification. *Biochem. Biophys. Res. Commun.* **441**, 886–890 (2013).

49. Leucht, P. *et al.* Wnt3a reestablishes osteogenic capacity to bone grafts from aged animals. *J. Bone Joint Surg. Am.* **95**, 1278–1288 (2013).

50. Leucht, P., Minear, S., Ten Berge, D., Nusse, R. & Helms, J. A. Translating insights from development into regenerative medicine: the function of Wnts in bone biology. *Semin. Cell Dev. Biol.* **19**, 434–443 (2008).

51. Huang, Y. *et al.* Inhibition of β-catenin signaling in chondrocytes induces delayed fracture healing in mice. *J. Orthop. Res.* **30**, 304–310 (2012).

52. Regard, J. B., Zhong, Z., Williams, B. O. & Yang, Y. Wnt Signaling in Bone Development and Disease: Making Stronger Bone with Wnts. *Cold Spring Harb. Perspect. Biol.* **4**, a007997 (2012).

53. Sarahrudi, K., Thomas, A., Albrecht, C. & Aharinejad, S. Strongly enhanced levels of sclerostin during human fracture healing. *J. Orthop. Res.* **30**, 1549–1555 (2012).

54. Canalis, E. Wnt signalling in osteoporosis: mechanisms and novel therapeutic approaches. *Nat. Rev. Endocrinol.* **9**, 575–583 (2013).

55. Janda, C. Y., Waghray, D., Levin, A. M., Thomas, C. & Garcia, K. C. Structural Basis of Wnt Recognition by Frizzled. *Science* **337**, 59–64 (2012).

56. Takada, R. *et al.* Monounsaturated fatty acid modification of Wnt protein: its role in Wnt secretion. *Dev. Cell* **11**, 791–801 (2006).

57. Willert, K. *et al.* Wnt proteins are lipid-modified and can act as stem cell growth factors. *Nature* **423**, 448–452 (2003).

58. Morrell, N. T. *et al.* Liposomal Packaging Generates Wnt Protein with In Vivo Biological Activity. *PLOS ONE* **3**, e2930 (2008).

59. Maes, C. *et al.* Placental growth factor mediates mesenchymal cell development, cartilage turnover, and bone remodeling during fracture repair. *J. Clin. Invest.* **116**, 1230–1242 (2006).

60. Zelzer, E. *et al.* Skeletal defects in VEGF(120/120) mice reveal multiple roles for VEGF in skeletogenesis. *Dev. Camb. Engl.* **129**, 1893–1904 (2002).

61. Matsubara, H. *et al.* Vascular tissues are a primary source of BMP2 expression during bone formation induced by distraction osteogenesis. *Bone* **51**, 168–180 (2012).

62. Yu, Y. Y. *et al.* Immunolocalization of BMPs, BMP antagonists, receptors, and effectors during fracture repair. *Bone* **46**, 841–851 (2010).

63. Nolan, D. J. *et al.* Molecular Signatures of Tissue-Specific Microvascular Endothelial Cell Heterogeneity in Organ Maintenance and Regeneration. *Dev. Cell* **26**, 204–219 (2013).

64. Rafii, S., Butler, J. M. & Ding, B.-S. Angiocrine functions of organ-specific endothelial cells. *Nature* **529**, 316–325 (2016).

65. Bhattacharjee, M. *et al.* Tissue engineering strategies to study cartilage development, degeneration and regeneration. *Adv. Drug Deliv. Rev.* **84**, 107–122 (2015).

66. Bourgine, P. E. *et al.* Osteoinductivity of engineered cartilaginous templates devitalized by inducible apoptosis. *Proc. Natl. Acad. Sci. U. S. A.* **111**, 17426–17431 (2014).

67. Dang, P. N. *et al.* Endochondral Ossification in Critical-Sized Bone Defects via Readily Implantable Scaffold-Free Stem Cell Constructs. *Stem Cells Transl. Med.* **6**, 1644–1659 (2017).

68. Farrell, E. *et al.* In-vivo generation of bone via endochondral ossification by in-vitro chondrogenic priming of adult human and rat mesenchymal stem cells. *BMC Musculoskelet. Disord.* **12**, 31 (2011).

69. Scotti, C. *et al.* Recapitulation of endochondral bone formation using human adult mesenchymal stem cells as a paradigm for developmental engineering. *Proc. Natl. Acad. Sci.* **107**, 7251–7256 (2010).

70. Scotti, C. *et al.* Engineering of a functional bone organ through endochondral ossification. *Proc. Natl. Acad. Sci. U. S. A.* **110**, 3997–4002 (2013).

71. Sheehy, E. J., Vinardell, T., Toner, M. E., Buckley, C. T. & Kelly, D. J. Altering the Architecture of Tissue Engineered Hypertrophic Cartilaginous Grafts Facilitates Vascularisation and Accelerates Mineralisation. *PLOS ONE* **9**, e90716 (2014).

72. Sheehy, E. J., Vinardell, T., Buckley, C. T. & Kelly, D. J. Engineering osteochondral constructs through spatial regulation of endochondral ossification. *Acta Biomater.* **9**, 5484–5492 (2013).

73. Nishitani, K. & Schwarz, E. M. Cartilage Transplants Hold Promise for Challenging Bone Defects. *Nat. Rev. Rheumatol.* **10**, 129–130 (2014).

74. Bjorn R. Olsen, Anthony M. Reginato & Wang, W. Bone Development. *Annu. Rev. Cell Dev. Biol.* **16**, 191–220 (2000).

75. Mandibular Fractures: Background, History of the Procedure, Epidemiology. (2015).

76. Yu, Y. Y., Lieu, S., Hu, D., Miclau, T. & Colnot, C. Site Specific Effects of Zoledronic Acid during Tibial and Mandibular Fracture Repair. *PLoS ONE* **7**, (2012).

77. Shapiro, I. M., Adams, C. S., Freeman, T. & Srinivas, V. Fate of the hypertrophic chondrocyte: microenvironmental perspectives on apoptosis and survival in the epiphyseal growth plate. *Birth Defects Res. Part C Embryo Today Rev.* **75**, 330–339 (2005).

78. Tsang, K. Y., Chan, D. & Cheah, K. S. E. Fate of growth plate hypertrophic chondrocytes: Death or lineage extension? *Dev. Growth Differ.* **57**, 179–192 (2015).

79. Park, K. H., Gu, D. R., So, H. S., Kim, K. J. & Lee, S. H. Dual Role of Cyanidin-3-glucoside on the Differentiation of Bone Cells. *J. Dent. Res.* 0022034515604620 (2015) doi:10.1177/0022034515604620.

80. Cunniffe, G. M. *et al.* Porous decellularized tissue engineered hypertrophic cartilage as a scaffold for large bone defect healing. *Acta Biomater.* **23**, 82–90 (2015).

81. Kumar, B. P., Venkatesh, V., Kumar, K. A. J., Yadav, B. Y. & Mohan, S. R. Mandibular Reconstruction: Overview. *J. Maxillofac. Oral Surg.* **15**, 425–441 (2016).

82. Wong, S. A. *et al.* Microenvironmental Regulation of Chondrocyte Plasticity in Endochondral Repair-A New Frontier for Developmental Engineering. *Front. Bioeng. Biotechnol.* **6**, 58 (2018).

83. Bahney, C. S. *et al.* Cellular biology of fracture healing. *J. Orthop. Res.* **37**, 35–50 (2019).

84. Silkstone, D., Hong, H. & Alman, B. A. β-Catenin in the race to fracture repair: in it to Wnt. *Nat. Clin. Pract. Rheumatol.* **4**, 413–419 (2008).

85. Bahney, C. S., Hu, D. P., Miclau, T. & Marcucio, R. S. The Multifaceted Role of the Vasculature in Endochondral Fracture Repair. *Front. Endocrinol.* **6**, (2015).

86. Zhou, X. *et al.* Chondrocytes transdifferentiate into osteoblasts in endochondral bone during development, postnatal growth and fracture healing in mice. *PLoS Genet.* **10**, e1004820 (2014).

87. Jing, Y. *et al.* Chondrocytes Directly Transform into Bone Cells in Mandibular Condyle Growth. *J. Dent. Res.* 0022034515598135 (2015) doi:10.1177/0022034515598135.

88. Gracanin, A. *et al.* Ligand-independent canonical Wnt activity in canine mammary tumor cell lines associated with aberrant LEF1 expression. *PloS One* **9**, e98698 (2014).

89. Aktary, Z., Bertrand, J. U. & Larue, L. The WNT-less wonder: WNT-independent β-catenin signaling. *Pigment Cell Melanoma Res.* **29**, 524–540 (2016).

90. Miravet, S. *et al.* Tyrosine phosphorylation of plakoglobin causes contrary effects on its association with desmosomes and adherens junction components and modulates beta-catenin-mediated transcription. *Mol. Cell. Biol.* **23**, 7391–7402 (2003).

91. Valenta, T., Hausmann, G. & Basler, K. The many faces and functions of β-catenin. *EMBO J.* **31**, 2714–2736 (2012).

92. Yang, W. *et al.* Nuclear PKM2 regulates β-catenin transactivation upon EGFR activation. *Nature* **480**, 118–122 (2011).

93. Krejci, P. *et al.* Receptor tyrosine kinases activate canonical WNT/β-catenin signaling via MAP kinase/LRP6 pathway and direct β-catenin phosphorylation. *PloS One* **7**, e35826 (2012).

94. Berg, T. *et al.* Fibroblast growth factor 10 is critical for liver growth during embryogenesis and controls hepatoblast survival via beta-catenin activation. *Hepatol. Baltim. Md* **46**, 1187–1197 (2007).

95. Mavila, N. *et al.* Fibroblast growth factor receptor-mediated activation of AKT-β-catenin-CBP pathway regulates survival and proliferation of murine hepatoblasts and hepatic tumor initiating stem cells. *PloS One* **7**, e50401 (2012).

96. Pai, R. *et al.* Inhibition of fibroblast growth factor 19 reduces tumor growth by modulating beta-catenin signaling. *Cancer Res.* **68**, 5086–5095 (2008).

97. Guvakova, M. A. & Surmacz, E. Overexpressed IGF-I receptors reduce estrogen growth requirements, enhance survival, and promote E-cadherin-mediated cell-cell adhesion in human breast cancer cells. *Exp. Cell Res.* **231**, 149–162 (1997).

98. Playford, M. P., Bicknell, D., Bodmer, W. F. & Macaulay, V. M. Insulin-like growth factor 1 regulates the location, stability, and transcriptional activity of beta-catenin. *Proc. Natl. Acad. Sci. U. S. A.* **97**, 12103–12108 (2000).

99. Morali, O. G. *et al.* IGF-II induces rapid beta-catenin relocation to the nucleus during epithelium to mesenchyme transition. *Oncogene* **20**, 4942–4950 (2001).

100. Esser, S., Lampugnani, M. G., Corada, M., Dejana, E. & Risau, W. Vascular endothelial growth factor induces VE-cadherin tyrosine phosphorylation in endothelial cells. *J. Cell Sci.* **111 (Pt 13)**, 1853–1865 (1998).

101. Cohen, A. W., Carbajal, J. M. & Schaeffer, R. C. VEGF stimulates tyrosine phosphorylation of beta-catenin and small-pore endothelial barrier dysfunction. *Am. J. Physiol.* **277**, H2038-2049 (1999).

102. Qi, J., Wang, J., Romanyuk, O. & Siu, C.-H. Involvement of Src family kinases in N-cadherin phosphorylation and beta-catenin dissociation during transendothelial migration of melanoma cells. *Mol. Biol. Cell* **17**, 1261–1272 (2006).

103. Gallagher, S. J. *et al.* Beta-catenin inhibits melanocyte migration but induces melanoma metastasis. *Oncogene* **32**, 2230–2238 (2013).

104. Conde-Perez, A. *et al.* A caveolin-dependent and PI3K/AKT-independent role of PTEN in β-catenin transcriptional activity. *Nat. Commun.* **6**, 8093 (2015).

105. Persad, S., Troussard, A. A., McPhee, T. R., Mulholland, D. J. & Dedhar, S. Tumor suppressor PTEN inhibits nuclear accumulation of beta-catenin and T cell/lymphoid enhancer factor 1-mediated transcriptional activation. *J. Cell Biol.* **153**, 1161–1174 (2001).

106. Galbiati, F. *et al.* Caveolin-1 expression inhibits Wnt/beta-catenin/Lef-1 signaling by recruiting beta-catenin to caveolae membrane domains. *J. Biol. Chem.* **275**, 23368–23377 (2000).

107. Mo, S. *et al.* Caveolin-1 regulates dorsoventral patterning through direct interaction with beta-catenin in zebrafish. *Dev. Biol.* **344**, 210–223 (2010).

108. Salomon, D. *et al.* Regulation of beta-catenin levels and localization by overexpression of plakoglobin and inhibition of the ubiquitin-proteasome system. *J. Cell Biol.* **139**, 1325–1335 (1997).

109. Li, L., Chapman, K., Hu, X., Wong, A. & Pasdar, M. Modulation of the oncogenic potential of beta-catenin by the subcellular distribution of plakoglobin. *Mol. Carcinog.* **46**, 824–838 (2007).

110. Simcha, I. *et al.* Differential nuclear translocation and transactivation potential of beta-catenin and plakoglobin. *J. Cell Biol.* **141**, 1433–1448 (1998).

111. Hausmann, G. & Basler, K. Wnt lipid modifications: not as saturated as we thought. *Dev. Cell* **11**, 751–752 (2006).

112. Kadowaki, T., Wilder, E., Klingensmith, J., Zachary, K. & Perrimon, N. The segment polarity gene porcupine encodes a putative multitransmembrane protein involved in Wingless processing. *Genes Dev.* **10**, 3116–3128 (1996).

113. van den Heuvel, M., Harryman-Samos, C., Klingensmith, J., Perrimon, N. & Nusse, R. Mutations in the segment polarity genes wingless and porcupine impair secretion of the wingless protein. *EMBO J.* **12**, 5293–5302 (1993).

114. Harada, N. *et al.* Intestinal polyposis in mice with a dominant stable mutation of the beta-catenin gene. *EMBO J.* **18**, 5931–5942 (1999).

115. Wang, Y. *et al.* Ephrin-B2 controls VEGF-induced angiogenesis and lymphangiogenesis. *Nature* **465**, 483–486 (2010).

116. Thompson, Z., Miclau, T., Hu, D. & Helms, J. A. A model for intramembranous ossification during fracture healing. *J. Orthop. Res. Off. Publ. Orthop. Res. Soc.* **20**, 1091–1098 (2002).

117. CRUZ-ORIVE, L. M. Unbiased Stereology: Three-Dimensional Measurement in Microscopy. *J. Anat.* **194**, 153–157 (1999).

118. Janda, C. Y. *et al.* Surrogate Wnt agonists that phenocopy canonical Wnt/β-catenin signaling. *Nature* **545**, 234–237 (2017).

119. Liu, W. *et al.* Deletion of Porcn in Mice Leads to Multiple Developmental Defects and Models Human Focal Dermal Hypoplasia (Goltz Syndrome). *PLOS ONE* **7**, e32331 (2012).

120. Ogata, K. *et al.* Identification and hematopoietic potential of CD45- clonal cells with very immature phenotype (CD45-CD34-CD38-Lin-) in patients with myelodysplastic syndromes. *Stem Cells Dayt. Ohio* **23**, 619–630 (2005).

121. McKinney-Freeman, S. L. *et al.* Surface antigen phenotypes of hematopoietic stem cells from embryos and murine embryonic stem cells. *Blood* **114**, 268–278 (2009).

122. de Lau, W. B., Snel, B. & Clevers, H. C. The R-spondin protein family. *Genome Biol.* **13**, 242 (2012).

123. Elliott, M. R., Koster, K. M. & Murphy, P. S. Efferocytosis signaling in the regulation of macrophage inflammatory responses. *J. Immunol. Baltim. Md 1950* **198**, 1387–1394 (2017).

124. Karaji, N. & Sattentau, Q. J. Efferocytosis of Pathogen-Infected Cells. *Front. Immunol.* **8**, (2017).

125. Monks, J., Smith-Steinhart, C., Kruk, E. R., Fadok, V. A. & Henson, P. M. Epithelial cells remove apoptotic epithelial cells during post-lactation involution of the mouse mammary gland. *Biol. Reprod.* **78**, 586–594 (2008).

126. Lööv, C., Mitchell, C. H., Simonsson, M. & Erlandsson, A. Slow degradation in phagocytic astrocytes can be enhanced by lysosomal acidification. *Glia* **63**, 1997–2009 (2015).

127. Golovchenko, S. *et al.* Deletion of beta catenin in hypertrophic growth plate chondrocytes impairs trabecular bone formation. *Bone* **55**, 102–112 (2013).

128. Willet, S. G. *et al.* Regenerative proliferation of differentiated cells by mTORC1-dependent paligenosis. *EMBO J.* **37**, (2018).

129. Galli, L. M., Zebarjadi, N., Li, L., Lingappa, V. R. & Burrus, L. W. Divergent effects of Porcupine and Wntless on WNT1 trafficking, secretion, and signaling. *Exp. Cell Res.* **347**, 171–183 (2016).

Publishing Agreement

It is the policy of the University to encourage open access and broad distribution of all theses, dissertations, and manuscripts. The Graduate Division will facilitate the distribution of UCSF theses, dissertations, and manuscripts to the UCSF Library for open access and distribution. UCSF will make such theses, dissertations, and manuscripts accessible to the public and will take reasonable steps to preserve these works in perpetuity.

I hereby grant the non-exclusive, perpetual right to The Regents of the University of California to reproduce, publicly display, distribute, preserve, and publish copies of my thesis, dissertation, or manuscript in any form or media, now existing or later derived, including access online for teaching, research, and public service purposes.

DocuSigned by:
Sarah Anne Wong
631891FE0AA8400...
Author Signature

6/1/2022
Date